Characterizing Emissions from Natural Gas Drilling and Well Completion Operations in Garfield County, CO

Prepared by:

Colorado State University

Department of Atmospheric Science

200 W. Lake St.

1371 Campus Delivery

Fort Collins, CO 80526-1371

June 14, 2016

Table of Contents

List of Figures

List of Tables

List of Acronyms and Abbreviations

APCD/CDPHE……….Air Pollution Control Division/Colorado Department of Public Health and Environment
BTEX…………………………………………………………………………….Benzene, Toluene, Ethylbenzene, and Xylenes
C_2H_2……Acetylene or Ethyne
CBL………………………………………………………………………………………………Convective Boundary Layer
CRDS………………………………………………………………………………………Cavity Ring-Down Spectroscopy
CSU……………………………………………………………………………………………………Colorado State University
EPA……………………………………………………………………………………………Environmental Protection Agency
ER………Emission Rate
FID…………………………………………………………………………………………………Flame Ionization Detector
GC………Gas Chromatography
GEOS-5……………………………………………………………..The Goddard Earth Observing System Model, Version 5
GPS………………………………………………………………………………………………Global Positioning System
$g\ s^{-1}$……………………………………………………………………………………………………..Grams per Second
HP………Hewlett Packard
LEL…………………………………………………………………………………………………..Lower Explosive Limit
LOD…………………………………………………………………………………………………..Limit of Detection
MFC…………………………………………………………………………………………………Mass Flow Controller
NARR…………………………………………………………………………………North American Regional Reanalysis
NCAR…………………………………………………………………………….National Center for Atmospheric Research
VOCs……………………………………………………………………………………Volatile Organic Compounds
ppbv…………………………………………………………………………………………..Parts Per Billion by Volume
SBL…………………………………………………………………………………………………Stable Boundary Layer
slpm………………………………………………………………………………………Standard Liters per Minute
TAC……………………………………………………………………………………………..Technical Advisory Committee
TRM……………………………………………………………………………………………………Tracer Ratio Method
USGS………………………………………………………………………………….United States Geological Survey
WAS…………………………………………………………………………………………………..Whole Air Samples

Executive Summary

Improved unconventional oil and natural gas extraction methods have facilitated the development of these resources in several areas, including the Piceance Basin of western Colorado. Increased activity has spurred questions concerning possible air pollutant emissions. Processes associated with natural gas extraction have been identified as emitting a variety of air pollutants, but the data available on the rates and types of compounds emitted are limited. This is especially true for emissions during drilling and completion (hydraulic fracturing and flowback) of new wells, activities which have not been closely studied for emission of atmospheric pollutants.

This study was designed to characterize and quantify emission rates and dispersion of air toxics, ozone precursors, and greenhouse gases from unconventional natural gas well development activities in Garfield County, CO, located on top of a geological formation known as the Piceance Basin. Particular focus was placed on quantifying emissions of individual volatile organic compounds (VOCs) and methane during well drilling, hydraulic fracturing ("fracking"), and flowback. While some prior studies have measured VOC or methane concentrations near well development operations, ambient concentrations are strongly dependent not only on emission rates but also on sampling location and meteorological conditions, which greatly affect downwind dispersion and dilution. By characterizing emission rates directly, results from this study can be used to predict downwind concentration fields for any location of interest under a wide range of weather conditions.

Emission rates were determined using a tracer ratio method (TRM). In this method, the rate of emission of a compound of interest (e.g., $g\ s^{-1}$ of benzene) is determined as the product of a known tracer emission rate multiplied by the ratio of the background-corrected concentrations of the compound of interest and the tracer. Acetylene was selected as a tracer gas and its controlled release co-located with the main source of emissions on studied well pads. Real-time methane and acetylene concentrations and three minute integrated whole air sample canisters for VOC analysis were collected downwind of the release location. Meteorological data were collected at two heights (3 m and 10 m) near the well pad. Upwind acetylene, methane, and VOC concentrations were determined for background correction. The canisters were analyzed for a large suite of VOCs using gas chromatography with flame ionization detection. The study results provide novel information concerning emissions from natural gas drilling and completion activities in Garfield County, CO and are some of the first measurements of this type in any U.S. basin. The number of experiments conducted for each operation type are reported in Table E.1.

Table E.1. Number of experiments conducted during this study for different types of operations.

Type of Operation	Number of experiments
Drilling	5
Fracking	5
Remote Fracking	1
Flowback	6
Fracking/Flowback	2
Drilling/Fracking/Flowback	1
Fracking/Workover/Flowback	1

Overall, 21 emission experiments were conducted from 2013-2015. Several sets of 2 to 5 canisters were collected at different times during each experiment, in addition to an upwind background sample per experiment. Using the TRM, each canister in the plume provides an independent measure of VOC emission rates. 28-48 VOCs are reported for each canister, along with real-time methane and acetylene data collected during each experiment. Using the TRM the emission rates of methane and individual VOCs are calculated and reported. Table E.2 shows median emission rates of methane and several key VOCs for each major operation type. Methane, ethane, and propane were the most abundant constituents in measured emissions. Generally, higher rates of VOC and methane emissions were observed during flowback operations, although a wide range of emissions was observed for each type of activity studied.

Table E.2. Median values of methane and select VOC emission rates from measurements during different operation types.

	Drilling Median (g s^{-1})	Fracking Median (g s^{-1})	Flowback Median (g s^{-1})
Methane	2.0	2.8	40
Ethane	0.13	0.088	0.93
Propane	0.12	0.013	0.37
i-Pentane	0.0070	0.00041	0.11
n-Pentane	0.0026	0.00027	0.081
Benzene	0.0037	0.029	0.062
Toluene	0.088	0.12	0.24
Ethylbenzene	0.00086	0.011	0.017
m+p-Xylene	0.0026	0.12	0.16

The emission rates and field observations were used to conduct air dispersion (using the EPA's AERMOD model) simulations to: (1) evaluate AERMOD's accuracy in predicting observed, near-field dispersion of VOCs in Garfield County, CO and (2) predict concentration fields, as a function of emission rate, for dispersion of a hypothetical compound under a range of local meteorological conditions at a site with terrain similar to that observed in Garfield County. While not perfectly designed for prediction of the short-term concentration fields measured in the study, AERMOD did a reasonable job predicting the observed extent of dispersion across several field experiments. Moreover, emission rate ranges determined by activity type in this study can be used in a wide range of future simulations with AERMOD or other models to simulate downwind concentration fields relevant to understanding potential local health and air quality impacts associated with well development activities in Garfield County.

The data collected during this study are available for public access at: (https://dspace.library.colostate.edu/handle/10217/172972). A more detailed and technical discussion of the study and its findings follows this summary.

List of Participants

Funding Sources:

Garfield County, CO
Encana Corporation
Ursa Resources Group
WPX Energy
Bill Barrett Corporation
Caerus Oil and Gas
Laramie Energy

Technical Advisory Committee:

Mr. Adam Berig, Encana Corporation
Mr. Gordon Pierce, APCD/CDPHE
Mr. Chad Schlichtemeier, Anadarko Petroleum Corporation
Dr. Gail Tonnesen, US EPA
Dr. Christine Wiedinmyer, NCAR

Project Research Team:

Colorado State University
Prof. Jeffrey L. Collett, Jr (PI)
Prof. Jay Ham (co-PI)
Prof. Jeffrey Pierce
Dr. Arsineh Hecobian
Dr. Andrea Clements
Ms. Kira Shonkwiler
Dr. Yong Zhou
Dr. Yuri Desyaterik
Mr. Landan MacDonald
Mr. Bradley Wells
Ms. Noel Hilliard

Air Resource Specialists
Mr. Mark Tigges
Mr. Bryan Bibeau
Mr. Christian Kirk

1. Introduction

1.1.   Background and Study Objectives

Garfield County is located in western Colorado, on top of the Piceance Basin where natural gas is trapped within shale/tight sand sedimentary formations below the surface. This basin is predominantly a gas producing province. Figure 1.1 shows the Uinta-Piceance Basin (in red) straddling Utah and Colorado with the outline of Garfield county plotted over the formation. According to a United States Geological Survey (USGS) assessment, more than 80% of the available natural gas in the Uinta-Piceance basin is in reservoirs that require the use of unconventional gas extraction methods for economically feasible results (Johnson et al., 2016).
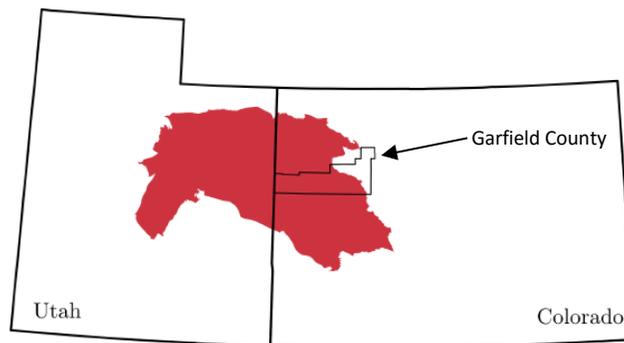
Figure 1.1. Map of Colorado and Utah, showing the Uinta-Piceance Basin in red. Garfield County is overlaid in black.

Unconventional oil and gas extraction methods such as horizontal drilling and hydraulic fracturing are frequently utilized to extract natural gas from low-permeability formations like tight sandstone and shale. The typical depth of a gas well is between 5000-9000 feet; after reaching a location near the shale formation, a directional drill is used for horizontal drilling for 5000 feet or more. Multiple horizontal wells accessing the same or other close by shale formations can be drilled from one pad. The drilling phase usually takes 4-10 days per well. After the drilling phase, hydraulic fracturing is used to inject water, sand, and chemicals into fractured sections of the well at high pressures. The fluid is used to open fractures further and connect them to create better pathways for more efficient flow of natural gas to the surface. Each well undergoes hydraulic fracturing in sections and each section is isolated with a cement plug. The hydraulic fracture phase of each well can span a period of 2-4 days. After the completion of hydraulic fracturing, the plugs are drilled out to enable the flow of fracking fluid, produced water, and natural gas up the well. This phase of well completion is known as flowback. The flowback water is typically stored on the pad and later transported for underground (well injection) storage or recycling and re-use in future hydraulic fracturing activities. The initial flowback period can last for 7-12 days per well, after which the fluid flow is reduced and the natural gas can be directed to storage or processed and directed to production sites and sales pipelines. The length of each stage (drilling, hydraulic fracturing, and flowback) can vary by site and is dependent on the number of wells planned for the pad.

Most of the production of natural gas in Garfield County is from sandstone lenses in the Williams Fork Formation. Technological advances in directional drilling and hydraulic fracturing have increased the

possibility of the production of gas from sandstone lenses (also referred to as tight sands). Garfield County experienced rapid growth in the number of natural gas producing wells between 1990 and 2014, raising public questions about air quality impacts. Quantifying the emission rates (ERs) and composition of emissions from natural gas development is a critical first step to evaluate potential impacts of air pollutants emitted from such activities in this region.

Colorado State University's (CSU's) Dr. Jeffrey L. Collett and Dr. Jay Ham proposed a study to characterize emissions from well development, which includes well drilling and completions operations. A variety of volatile compounds can be released to the atmosphere from these processes. The primary focus of the study is to characterize emissions of air toxics, ozone precursors, and greenhouse gases from various stages of well development in Garfield County, CO. Specifically, the study examined emission rates of methane and a wide range of individual volatile organic compounds (VOCs) and their near-field dispersion. The study was funded by an intergovernmental agreement between Colorado State University and Garfield County with gifts provided in support of the study from several industry partners: Encana Corporation, WPX Energy, Ursa Resources Group, Bill Barrett Corporation, Caerus Oil and Gas, and Laramie Energy. As part of the study, a Technical Advisory Committee (TAC) was assembled. The CSU team, with input from the TAC, prioritized the type and number of experiments and sites. TAC members were updated on the progress of the study and their input was incorporated in evaluating the direction and progress of the study throughout the project.

The approach used for the field measurements is described in Section 2. Briefly, the CSU team worked with several industry partners to identify sites with drilling, hydraulic fracturing, or flowback activity available for characterization. Site selection criteria also included local terrain and accessibility for downwind measurements. The Tracer Ratio Method (TRM), described by Lamb et al. (1995), was used to quantify emission rates (ERs) of VOCs from natural gas well development activities. In this approach, a conservative tracer is co-located with the source of interest and emitted at a controlled rate. The rate of emission of a compound of interest (e.g., g s^{-1} of benzene) is determined as the product of the tracer emission rate multiplied by the ratio of the background-corrected concentrations of the compound of interest and the tracer. Through this technique, the complex dispersion and dilution that occurs during turbulent transport from the emissions point to the measurement point is directly accounted for by the dilution of the tracer. A tracer release system (Section 2.2.1) was stationed on the pad and co-located with the major identified emission source. A tracer gas (acetylene) was emitted at a known flow rate. CSU's mobile plume tracker, equipped with an analyzer (Picarro Cavity Ringdown System) for the real-time measurement of methane and acetylene (Section 2.2.2), was deployed downwind of the pad to detect the tracer gas and locate the plume. When a plume was identified, evacuated Silonite® coated stainless steel canisters were remotely triggered (Section 2.2.4) to collect whole air samples for 3 minutes. The sampled canisters were transported to CSU for subsequent VOC analysis using Gas Chromatography with Flame Ionization Detection (GC-FID) (Section 2.2.5). Measurements were also made upwind of the pad to determine background concentrations. The real-time methane and acetylene data (Section 2.3.1) and the canister VOC data (Section 2.3.2) were analyzed to determine the ERs of methane and VOCs from each study site and activity. Use of the background methane and VOC data in the ER calculations ensured

that the identified emissions were limited to those associated with targeted activity on the pad. Emission results are presented in Sections 3.1 and 3.2.

The EPA dispersion model AERMOD was used to model the dispersion of emissions at each study site in order to compare predicted concentration fields with those observed, providing an assessment of the accuracy of the model predictions. AERMOD was also run over a longer period at a typical site with terrain characteristic of Garfield County, CO to simulate how near-field concentrations of compounds of interest are predicted to vary over a range of typical meteorological conditions. AERMOD model parameters are described in Section 2.3.5 and the results from the modeling analyses are presented in Section 3.3.

1.2.   Overview of Sample Collection

1.2.1. Site Selection

Members of the CSU research team worked with the study's industry partners to identify Garfield County locations where drilling, hydraulic fracturing, or flowback activities were planned. Once potential sites were identified, local terrain and meteorological conditions typical of the pad were investigated and the accessibility of the area surrounding the site with the plume tracker vehicle was examined. Given low natural gas prices, which persisted during most of the three year study period, the number of new wells being developed dropped significantly over the course of the study and each available site was carefully considered for study inclusion. Whenever possible, sites were selected where only a single operation was underway: drilling, fracking, or flowback. Due to extremely limited site availability, a few sites were included where simultaneous operations were being conducted.

1.2.2. Equipment Setup

For each emission experiment, the meteorological station (Section 2.2.3), the mobile plume tracker (A Hybrid Chevy Tahoe, see Section 2.2.2), and the tracer release system (2.2.1) were positioned on and around the pad, with the tracer release system being co-located with the primary point of emissions for a particular activity. The meteorological station was usually positioned upwind of the pad. Figure 1.2 is an overview of the equipment setup at a typical site.
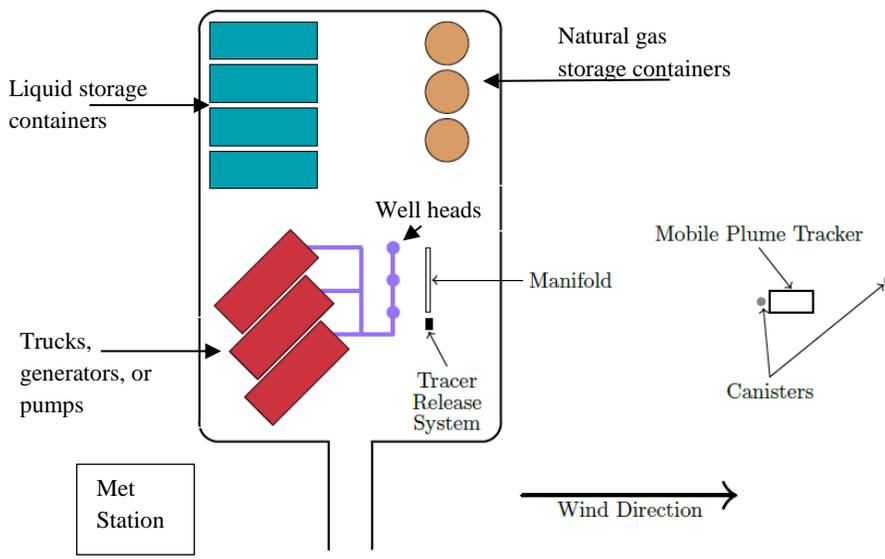
Figure 1.2. Overview of equipment setup at a typical site, adapted from MacDonald (2015).

1.2.3. Sampling Overview

The tracer gas was released from the system on the pad, when meteorological conditions stabilized and appeared favorable for a successful experiment. The plume tracker vehicle was driven downwind of the pad to locate the plume. Once the plume was located, the plume tracker vehicle would stop and three evacuated canisters would be deployed (two near the vehicle and one closer/farther from the pad, on a tripod). Using remote triggering systems, the canisters would be triggered simultaneously to collect ambient air for 3 minutes. At the conclusion of the sample collection, new canisters would be attached and ready for the next set of sample collection. Typically, 4 sets of 3 canisters were collected at each site. Table 1.1 presents information on the site operation type, number of canisters and sets of canisters collected from each site. As is evident from the table, 4 sets of 3 canisters were not always deployed at each site. Variations are due to changes made because of meteorological conditions, changes in site operations, or terrain conditions downwind of the pad.

Table 1.1. Number of experiments and information on operation types, number, and sets of canisters collected.

Experiment #	Type of Operation	Number of Canisters (including background)	Sets of Canisters (number of measurement periods)
1	Drilling	14	2
2	Drilling	17	3
3	Fracking	8	2
4	Drilling	7	3
5	Drilling	5	2
6	Remote Fracking	5	4
7	Fracking	18	6
8	Flowback	22	7
9	Fracking	2	1
10	Fracking, Flowback, and Workover	2	1
11	Flowback	10	4
12	Drilling	13	4
13	Drilling, Fracking, and Flowback	10	3
14	Fracking	10	3
15	Fracking	11	4
16	Flowback	12	4
17	Flowback	16	5
18	Fracking and Flowback	6	2
19	Flowback	19	6
20	Flowback	13	6
21	Fracking and Flowback	19	6

For each site visited, at least one canister was collected immediately upwind of the site to represent background concentrations of VOCs at that site. This background correction ensures that reported emissions reflect only those emissions from the well pad being studied and does not include emissions from other nearby or regional sources. Usually, acetylene was released at the time of background collection and the mobile plume tracker was used to ensure that no above-background acetylene was observed during the collection of the background canister. It was assumed that the upwind canister was representative of the background concentrations of VOCs for each experiment.

2. Measurement Methods

2.1. Tracer Ratio Method

The TRM is a straightforward technique that requires access to the emission source and involves the release of a passive tracer gas co-located with the source of emissions. The known ER of the tracer gas is multiplied by the ratio of the downwind concentrations of the emitted gas to the tracer gas (both in excess of background) to determine the ER of the gas of interest. The TRM has been used as a technique for estimating the ERs of gases from a variety of sources (e.g., Lamb et al., 1986; Lassey et al., 1997; Rumburg et al., 2008; Scholtens et al., 2004). In this study, acetylene (also known as ethyne, C_2H_2) was used as the

tracer gas. Acetylene was chosen because of its chemical stability, relatively long lifetime in the atmosphere (~2 weeks), ease of detection at high time resolution and low concentrations, and absence as a major emission of oil and gas operations.

The following equation was used to calculate the ERs of VOCs,

$$Q_{VOC} = Q_{C_2H_2} * \frac{[VOC]}{[C_2H_2]}$$

where, Q_{VOC} is the ER of the desired species, $Q_{C_2H_2}$ is the (known) release rate of acetylene, $[VOC]$ and $[C_2H_2]$ are the background-corrected concentrations of the emitted gas (VOC) and the tracer gas (acetylene), respectively. The concentrations can be integrated over space and/or time depending on the type of analysis performed. In this study, both the instantaneous and time integrated concentrations were used during data analysis. The instantaneous concentrations were used for estimating ERs of methane and the time integrated concentrations were used to report the ERs of VOCs. The basic assumptions of TRM are:

- The ER of the tracer is accurately known.
- The concentrations measured downwind are accurate.
- The two gaseous species disperse in a similar manner.
- The tracer is co-located with the emission source being characterized.
- Neither the tracer, nor the target VOC are altered by deposition or chemical reaction between the release and detection points.

In order to evaluate the accuracy of this method, several controlled release experiments were conducted where acetylene and methane were collocated and released at known ERs. TRM was used to estimate the ER of methane and the results were compared with the known values to determine the method uncertainty. Wells (2015) provides a detailed description of these experiments. The TRM method uncertainty in the controlled release experiments (Wells et al., 2016) was characterized by an accuracy (mean bias) of +22.6% and a precision of ±16.7% (relative standard deviation). As shown in Table 2.1, the precision reported here is similar to values reported from other studies. The accuracy and precision of the TRM method are considered more than acceptable, particularly given the large variability in actual emission rates observed in study field experiments. The precision of the TRM was also evaluated for individual VOC emission rates using replicate canister measurements collected during the field study; precision varied between approximately 0.2 and 98% (relative standard deviation) for individual VOCs, with most values less than 25%.

Table 2.1. TRM method precision reported by various studies.

Study	Precision (%)
Lamb et al. (1995)	±15
Kaharabata & Schuepp (2000)	±30
Galle et al. (2001)	±15 to ±30
Scholtens et al. (2004)	-25 to +43
Mønster et al. (2014)	±5
This study (Wells et al., 2016)	±17

2.2.   Measurement Techniques

2.2.1. Tracer Release System

A tracer release system was designed to ensure consistent, quantified, and safe release of the acetylene near the pre-identified main source of emissions on the well pad. This system consisted of three acetylene cylinders that were connected in parallel to a regulator to ensure pressure equilibration in each cylinder and to prevent the release of liquid acetone from the acetylene tank into the regulator and the lines. The regulator controlled the pressure of acetylene as it entered the attached Bev-A-Line IV non-reactive plastic tubing. An Alicat M-Series Mass Flow Controller (MFC) was used to regulate the acetylene flow, which allowed the appropriate mass flux of gas to enter a mixing chamber. The acetylene gas was diluted with ambient air to keep the concentrations below the Lower Explosive Limit (LEL). The diluted tracer gas was then transported via an accordion hose to a 6 m-long perforated manifold, held ~4m above ground on aluminum tripods, for release. Generally, release flow rates of at least 10 standard liters per minute (slpm) were utilized to ensure the concentrations observed downwind were adequately above background levels. A Campbell Scientific CR850 Data Logger was used to record the temperature, pressure, and acetylene mass flow rate as a function of time at 1 Hz. Figure 2.1 is a diagram of this system and Figure 2.2 is a photo of the system as deployed in the field.
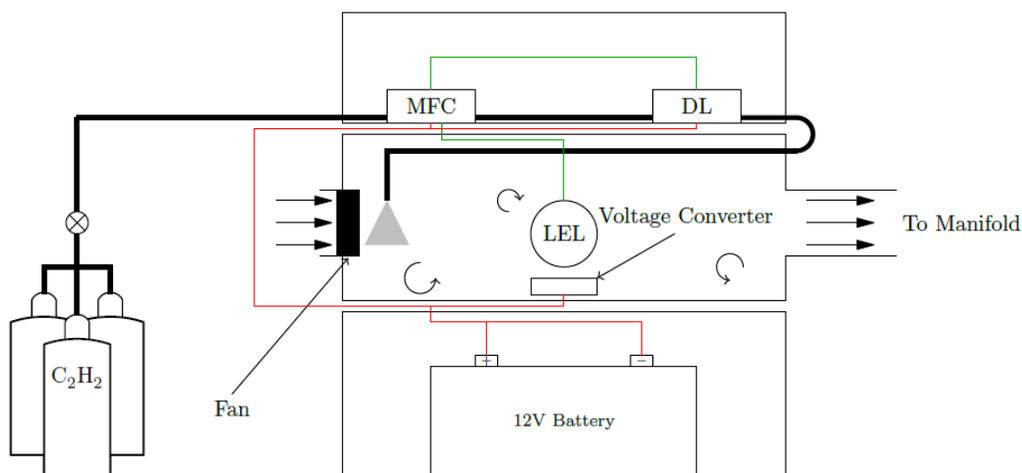

Figure 2.1. Diagram of the tracer release control system and C_2H_2 cylinders adapted from Wells et al. (2016). Acetylene cylinders are connected to a mass flow controller (MFC) and directed to a mixing box with a lower explosive limit (LEL) detector. The acetylene is then directed to a perforated manifold for release to the atmosphere as presented in Figure 2.2.
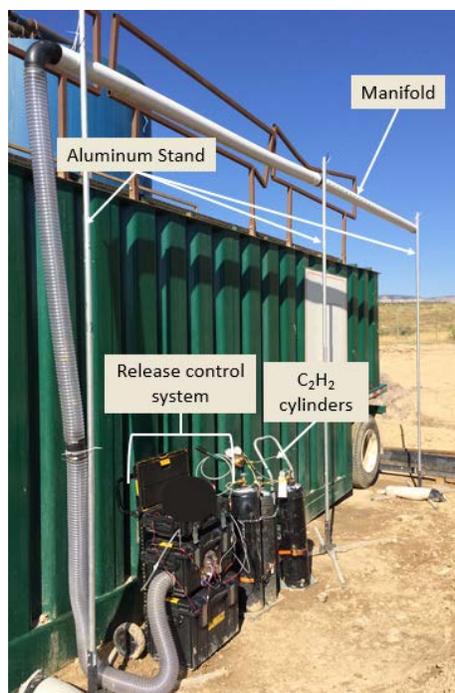
Figure 2.2. Photo of the tracer release system as deployed in the field. The C_2H_2 cylinders and the tracer release control system are presented in Figure 2.1.

2.2.2. Mobile Plume Tracker

Downwind of the tracer release system, a mobile plume tracker was deployed to measure the concentration of acetylene (the tracer gas) and methane. This system consisted of a Chevrolet Tahoe hybrid sport utility vehicle that housed a Picarro G2203 analyzer and A0931 mobile measurement kit that collected data on the concentrations of methane and acetylene using cavity ring-down spectroscopy (CRDS). The instrument inlet was located at a height of 3 m in the front of the SUV and was connected to the analyzer using ~4.5 m Teflon® tubing which directed ambient air into the Picarro system at 5 L min^{-1}. Adjacent to the Picarro inlet was a Global Positioning System (GPS) and an All-In-One meteorological sensor for wind speed and wind direction measurements. The data from the analyzer were displayed inside the plume tracker vehicle in real-time. Table 2.2 summarizes the measurement capabilities of this system.

Table 2.2. Instrument description and measurement capabilities of the mobile plume tracker.

Instrument Type	Model	Manufacturer	Measurement Interval
CRDS methane and acetylene analyzer	G2203	Picarro	3Hz
Mobile computer for analyzers	A0931	Picarro	3Hz
GPS	A21	Hemisphere GNSS	3Hz
Wind speed and direction	102779-A1-C1-D0	Climatronics	3Hz

The mobile plume tracker was used to obtain simultaneous information about the spatial and temporal variability of methane and acetylene concentrations to determine the ER of methane and map the location of the plume from the pad. In addition to the instruments noted above, the mobile plume tracker housed two of the three remote canister triggering systems deployed for whole air sample (WAS) collections. A complete description of the triggering systems is presented in Section 2.2.4. Figure 2.3 presents a photo of the mobile plume tracker and its various parts; the analyzers and the computer are housed inside the vehicle.

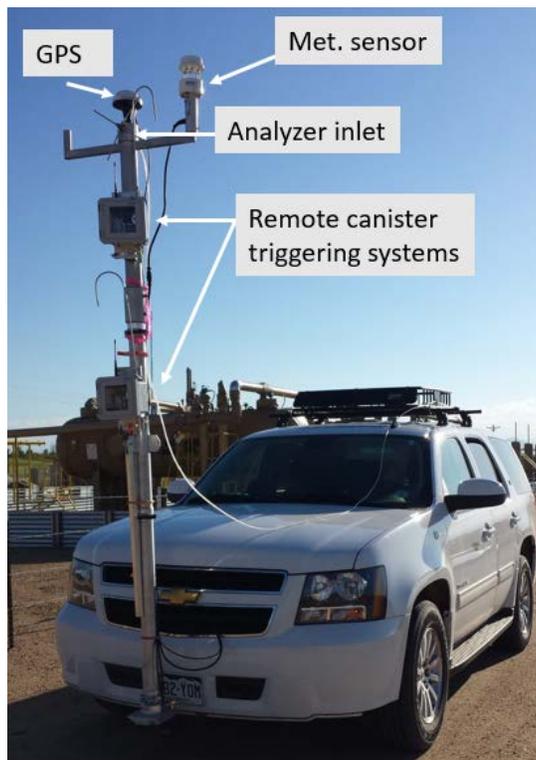*Figure 2.3. Mobile plume tracker with its external components for plume identification and sampling.*

2.2.3. Meteorological Station

Meteorological variables (high temporal resolution 3D wind vectors, temperature, relative humidity, and pressure) were measured at two heights (3 m and 10 m) for the duration of each experiment. Figure 2.4 is a photo of the meteorological station as deployed in the field.
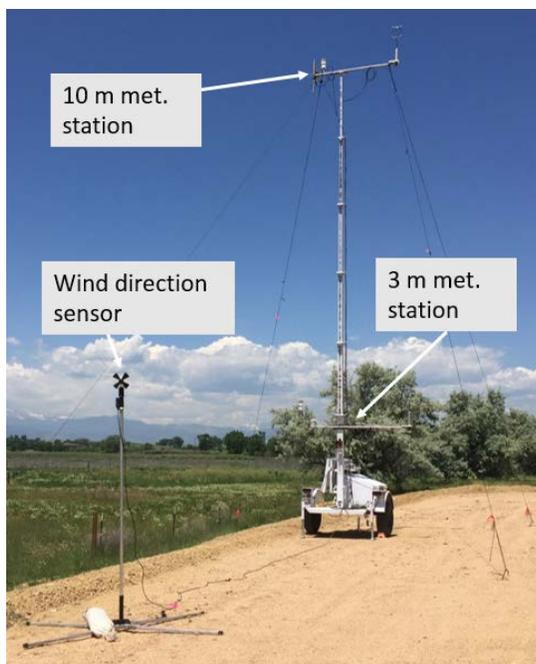
Figure 2.4. Picture of the meteorological station used for measurements during this study.

A summary of the meteorological instruments that were used and the type of data collected are given in Table 2.3.

Table 2.3. Instruments used for the collection of meteorological data.

Instrument Type	Model	Manufacturer	Measurements
Sonic Anemometer	WindMaster	Gill	3D wind vectors, temperature, and water vapor concentrations
Weather Station	All-In-One	Climatronics	2D wind vectors, temperature, pressure, and relative humidity
Wind Monitor	05103	R. M. Young	Wind direction and speed
Data Logger	CR1000	Campbell Scientific	Data acquisition and storage

2.2.4. Canister Triggering System

Evacuated 1.4 L Silonite®-coated stainless steel canisters (Entech Instruments, Simi Valley, CA) coupled with remote triggering systems (Air Resource Specialists, Fort Collins, CO), were used for the collection of whole air samples. Typically, three canisters were deployed for each sample period: two were positioned adjacent to the mobile plume tracker at different heights and a third canister was positioned either further downwind or upwind of the mobile plume tracker based on the terrain and general layout of the site. The location of the triggering systems with respect to the mobile plume tracker is shown in Figure 2.3. The third canister was positioned on a tripod about 2m above ground. Figure 2.5 is a photo of the third canister triggering system and its components.

20
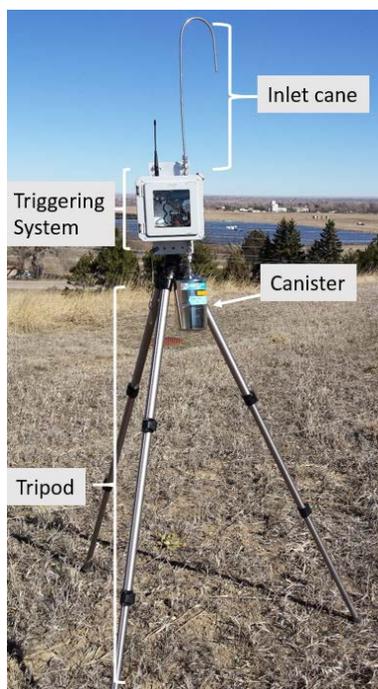
Figure 2.5. Photo of the third canister triggering system and its components, deployed on a tripod.

The triggering systems were outfitted with an Arduino UNO microcontroller controlled solenoid valve that was opened for a total of 180 seconds to allow ambient air to be trapped in the canister for later analysis. A pressure sensor, GPS, and temperature sensor were placed within the fiberglass enclosure of the triggering system. A detailed list of the components is found in Table 2.4. A custom LabVIEW interface remotely activated the triggering systems to open simultaneously using a portable netbook computer.

Table 2.4. List of components from the canister remote triggering system (Air Resource Specialists, Fort Collins, CO).

Component	Model	Manufacturer
Microcontroller	UNO	Arduino
GPS	PMB-688	Polstar
Temperature Sensor	LM35	Texas Instruments
Wireless Modem	XBee-PRO 900HP	Digi
Pressure Sensor	OEM 0-15 PSIA	Honeywell
Solenoid Valve	S311PF15V2AD5L	GC

2.2.5. Canister VOC Measurement System

2.2.5.1 Canister Cleaning System

The 1.4 L Silonite® coated canisters (Entech) were cleaned before each field deployment using an Entech 3100 Canister cleaning system following procedures outlined in EPA's TO-15 method. Each set of canisters included a batch blank, which was analyzed for VOCs for quality assurance.

2.2.5.2. Canister Analysis Setup

The WAS were analyzed to identify and quantify 28 or 48 VOCs of interest. Procedures similar to EPA's TO-12 method were followed for this analysis. The WAS were cryogenically pre-concentrated and analyzed using one of two GC-FID systems. At the beginning of the study, a Hewlett Packard (HP) GC-FID system, coupled with an Entech pre-concentration unit, was used for cryogenic trapping and the subsequent analysis of VOCs. About 20% of the canister data presented in this report were analyzed using this system for 28 VOCs. A few months after the beginning of the study a different system for the analysis of VOCs was obtained, which enabled us to analyze a suite of 48 VOCs. Canister sample analytes were cryogenically pre-concentrated similar to the HP GC-FID procedure before being directed to a multi-channel GC system. Chromatograms from the channels that were equipped with FIDs were used for the analysis of the data presented here. After the acquisition of the multi-channel system, all WAS were analyzed using the new system because it is more sensitive for most VOCs when compared to the HP GC-FID system and 20 more VOCs could be quantified. Swarthout (2014) presents a detailed description of this multi-channel system.

Each GC-FID system was calibrated using dilutions of a 1 ppm Linde Gas certified high pressure standard. Six clean canisters, filled with ultra-high purity nitrogen, were analyzed to calculate the limit of detection (LOD) of each system. The results of calibration tests and LODs for each system are presented in Tables B.1 and B.2 in Appendix B.

2.3. Data Analysis

2.3.1. Real-Time Methane and Acetylene

Real-time methane and acetylene data were used to calculate a point-by-point distribution of methane ERs. In order to accurately calculate the ERs, background concentrations of methane and acetylene were subtracted from the measured concentrations. Background concentrations of acetylene in Garfield County were relatively low (0-0.8 ppbv) compared to the tracer signal (typically > 50 ppbv). The background concentration of acetylene did not change significantly with time and thus the average of the lowest 5% of values was used for each experiment. To address variability in the methane background, an interpolated background was used. When the detected acetylene concentrations were at background (i.e. out-of-plume), the methane concentrations were also considered out-of-plume. The background methane concentrations during each of these out-of-plume time periods were quantified. During in-plume time periods, the methane background was assumed to change linearly with time. To address the temporal variability of the measured plume acetylene concentrations, Butterworth low-pass smoothing was performed on the data using a cutoff frequency of 0.005 s^{-1}. Once the data had been background corrected, TRM was performed on a point-by-point basis. This produced distributions of ERs for each measurement period of each operation type. Not all methane and acetylene data collected during the study were included in calculations of final ER distributions. TRM was performed only when all of the following criteria were met:

- Mobile plume tracker was stationary.
- Tracer release system was set to be releasing more than 1 slpm of acetylene.
- Acetylene was above a lower cutoff value of 0.8 ppbv (ensuring we were well within the tracer plume).
- Correlation coefficient, r, of methane and acetylene concentrations was above 0.5 (ensuring co-location of the tracer and site emission plumes).

2.3.2. Canister VOCs

The acetylene concentrations within the canisters were evaluated to assess whether a canister was collected inside or outside of a plume. Canister samples were discarded if the acetylene concentration was less than 2 ppbv. This acetylene cutoff was selected by adding the average and one standard deviation of the C_2H_2 background concentrations for all canisters collected during the study. The mean C_2H_2 background concentration for all background samples collected during the study was 0.72 ppbv and the standard deviation of all of the C_2H_2 background concentrations was 0.89 ppbv. The ranges of background concentrations for all VOCs from background canisters collected throughout the study are presented in Appendix A. In some instances, VOC concentrations were below the GC-FID limit of detection (LOD), in which case the measured value was replaced with LOD/2 for the corresponding analysis system and VOC. The LODs for each system and each VOC are presented in Appendix B. Canister VOC data were then background corrected. The background correction involved subtracting the concentrations measured from the background canister deployed upwind of the emission location from the VOC values in the sampled canister. In cases where the background was equal to or higher than the measured concentration of a VOC, the determined value was replaced with LOD/2 for the corresponding analysis system and VOC. After processing the concentrations of the VOCs found in the downwind canister samples, the ERs of the VOCs were calculated using the TRM method as described in Section 2.1.

2.3.3 Dispersion Modeling using AERMOD

AERMOD is an atmospheric dispersion model approved by USEPA and frequently used to characterize the impact of a new emission source (Cimorelli et al., 2004). It has the ability to incorporate complex terrain, feature multiple sources and receptors, and determine downwind concentration fields within 50 km of the source. AERMOD disperses plumes using hourly averaged meteorology. It assumes the plume to be Gaussian within both the stable boundary layer (SBL) and in the convective boundary layer (CBL). AERMOD was used in this study for two analyses: (1) to replicate the time/location of each field measurement using a combination of field meteorological measurements and reanalysis data to compare AERMOD predicted concentration fields with ambient concentration measurements, and (2) to simulate a distribution of expected concentrations, per unit emission rate, for a site location typical of Garfield County using archived meteorological fields, with model run simulations which were one year long. The former application is intended to evaluate the ability of AERMOD to accurately predict air pollutant dispersion under conditions observed during this study, while the latter application is intended to illustrate AERMOD capabilities for future prediction of air pollutant concentration fields associated with activity emission rates determined in this study. Table 2.5 presents the meteorological variables that are required to run AERMOD. This table summarizes the source(s) of the data used here depending on the application.

Table 2.5. List of atmospheric variables required to run AERMOD. The sources of the variables are given based on the application.

Variables	Site-Specific Simulation	Annual Simulation
Surface Temperature	Study Met-Station	NARR
Surface Pressure		
Sensible Heat Flux		
Surface Wind Vector		
Friction Velocity		
Convective Velocity Scale		
Moni-Obukhov Length		
Planetary Boundary Layer	NARR (North American Regional Reanalysis)	
Bowen Ratio		
Vertical Potential Temperature Gradient above PBL		
Albedo		
Vertical Temperature Profile		
Vertical Wind Vector Profile		
Surface Roughness	GEOS-5 (The Goddard Earth Observing System Model, Version 5)	

3. Results

3.1. Methane ERs

The ER distributions of methane for all the real-time data collected across all processes during this study are shown in Figure 3.1. The x-axis is the ER determined from the TRM on a log-scale and the y-axis is the normalized frequency distribution calculated in log-space.   Approximately 60,000 total measurements were made across all experiments, representing a total in-plume measurement time of 5.6 hr. The overall methane ER distribution for all operations is bimodal and the complete dataset spans 6 orders of magnitude. The majority of methane emission rates fall between 1 and 100 g s^{-1}; the mean and median values for the full dataset are 103.6 and 55.8 g s^{-1}, respectively.
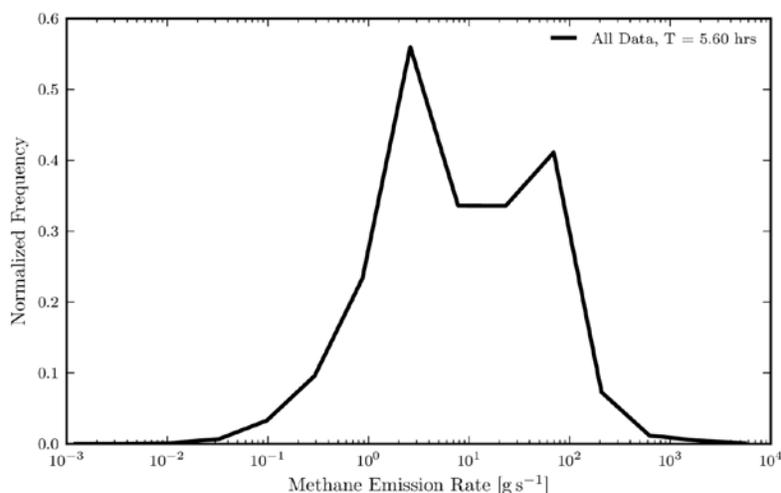

Figure 3.1. Normalized frequency distribution of all real-time methane emissions data collected during the study. T indicates the total number of hours of data available, representing approximately 60,000 individual measurements collected at a frequency of 3 Hz across the full set of study experiments.

The methane ER data were separated based on operation type as outlined in Table 1.1. Figure 3.2 shows separate distributions of methane ERs for each type of operation including drilling, fracking, flowback, and simultaneous operations. Table 3.1 summarizes the results in Figure 3.2. For the drilling, fracking, and the combination of fracking/workover/flowback activities methane ERs centered near 1-5 g s^{-1} and flowback, fracking/flowback, and drilling/fracking/flowback activities had progressively higher distribution centers. Most of the operations that include flowback show a bimodal distribution for methane ER. One site was visited where remote fracking operations were in progress. Data from this site were not reported as the acetylene cutoff and the acetylene-methane correlation coefficient requirements were not met.
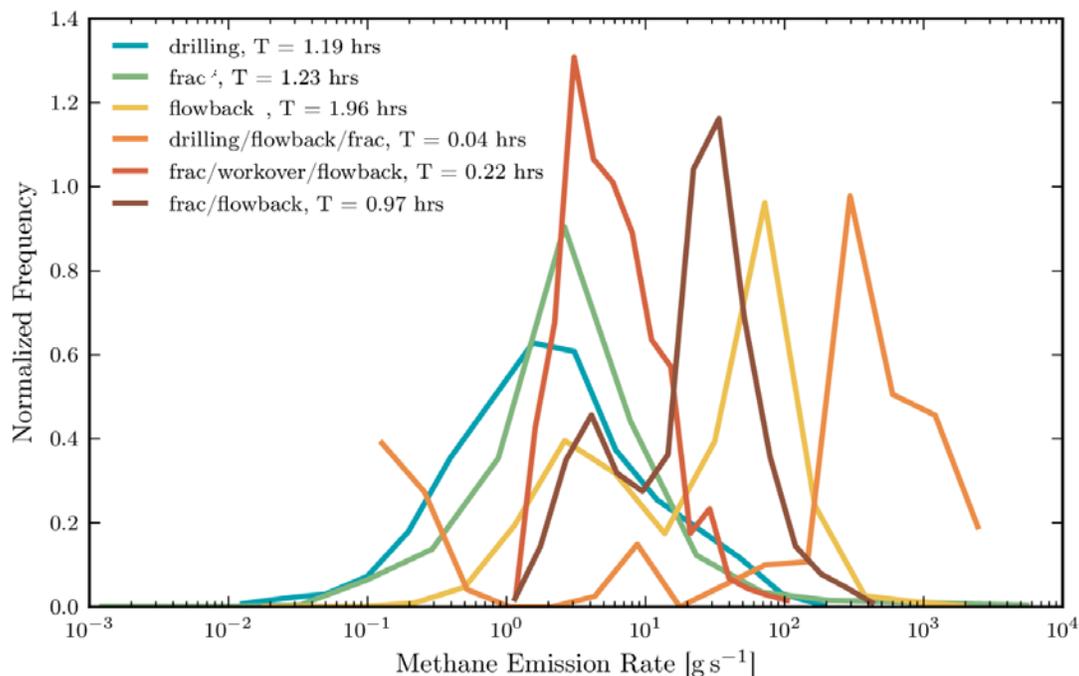

Figure 3.2. Methane ER distributions by operation type. T indicates the total amount of time when data were collected across all experiments for each operation type at a frequency of 3 Hz.

Continuous distributions of methane ER are most evident for drilling and hydraulic fracturing operations, with median emission rates of 2.0 and 2.8 g s^{-1} for these two activities, respectively. The fracking emissions data represent a range of sites that employed a variety of hydraulic fracturing techniques. Methane emission rates from flowback show a more complex, bimodal distribution. These emissions are generally larger than those seen from drilling and fracking operations, with a median value of 40 g s^{-1}. The methane ERs for several individual experiments are plotted on separate graphs and presented in figures in Appendix C.

Table 3.1. ER distributions of methane calculated using the TRM. The data are separated into their respective operation types.

Operation Type	# of Experiments	T (hrs)	Mean (g s⁻¹)	Median (g s⁻¹)	25th %ile (g s⁻¹)	75th %ile (g s⁻¹)
Drilling	5	1.2	6.5	2.0	0.73	5.3
Fracking	5	1.2	29	2.8	1.4	5.5
Flowback	6	2.0	54	40	4.3	77
Drilling/Fracking/Flowback	1	0.036	490	260	11	560
Fracking/Workover/Flowback	1	0.22	8.1	5.1	3.2	9.2
Fracking/Flowback	2	0.97	34	25	8.5	41

3.2. VOC ERs

Figure 3.3 depicts the distribution of 48 VOC ERs for all the canisters collected and presented in this report. This includes all operation types and all measurement periods where quality control criteria were satisfied. The y-axis is log scaled, as the range of VOC ERs spans several orders of magnitude. Table 3.2 presents a statistical summary of the ER data in Figure 3.3 for select VOCs.
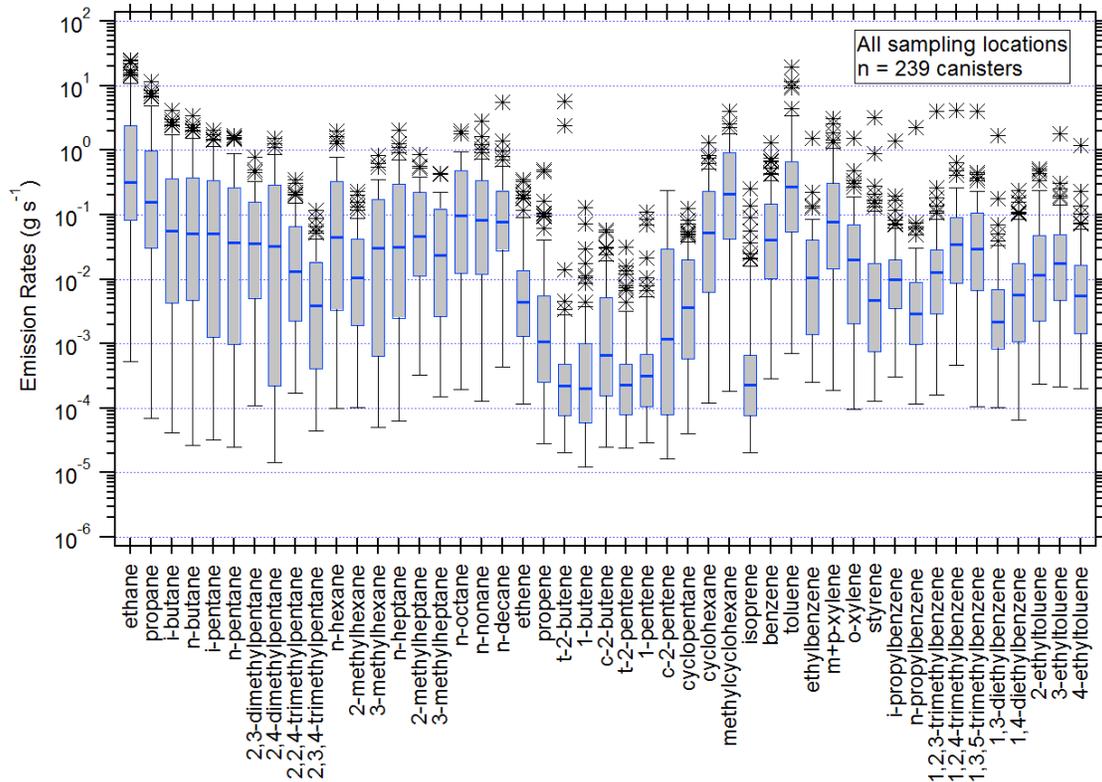

Figure 3.3. ERs of VOCs from canisters collected from all sites and operations during the study. The bottom and top of the boxes are the 25th and 75th percentiles, the blue line inside the box represents the median, the bottom and top whiskers are the 5th and 95th percentiles, and the stars are outliers beyond the 5th and 95th percentiles.

Table 3.2. Mean, median, 25th percentile and 75th percentile of the data for a subset of VOCs for all canisters collected during all operations for the study.

VOC	Mean (g s⁻¹)	Median (g s⁻¹)	25th %-ile (g s⁻¹)	75th %-ile (g s⁻¹)
Ethane	2.13	0.31	0.080	2.35
Propane	0.86	0.15	0.030	0.95
i-Pentane	0.23	0.050	0.0013	0.34
n-Pentane	0.19	0.037	0.00098	0.26
n-Decane	0.19	0.078	0.028	0.24
Ethene	0.019	0.0044	0.0013	0.013
Propene	0.012	0.0011	0.00025	0.0055
Benzene	0.10	0.040	0.010	0.14
Toluene	0.81	0.27	0.054	0.67
Ethylbenzene	0.032	0.010	0.0014	0.40
m+p-Xylene	0.23	0.076	0.014	0.30
o-Xylene	0.057	0.020	0.0020	0.071

In order to provide insight into the ERs of VOCs during different operations, ERs were grouped based on operation type and the data presented in separate figures for each operation based on the information in Table 1.1. Data from all drilling operations are presented in Figure 3.4.
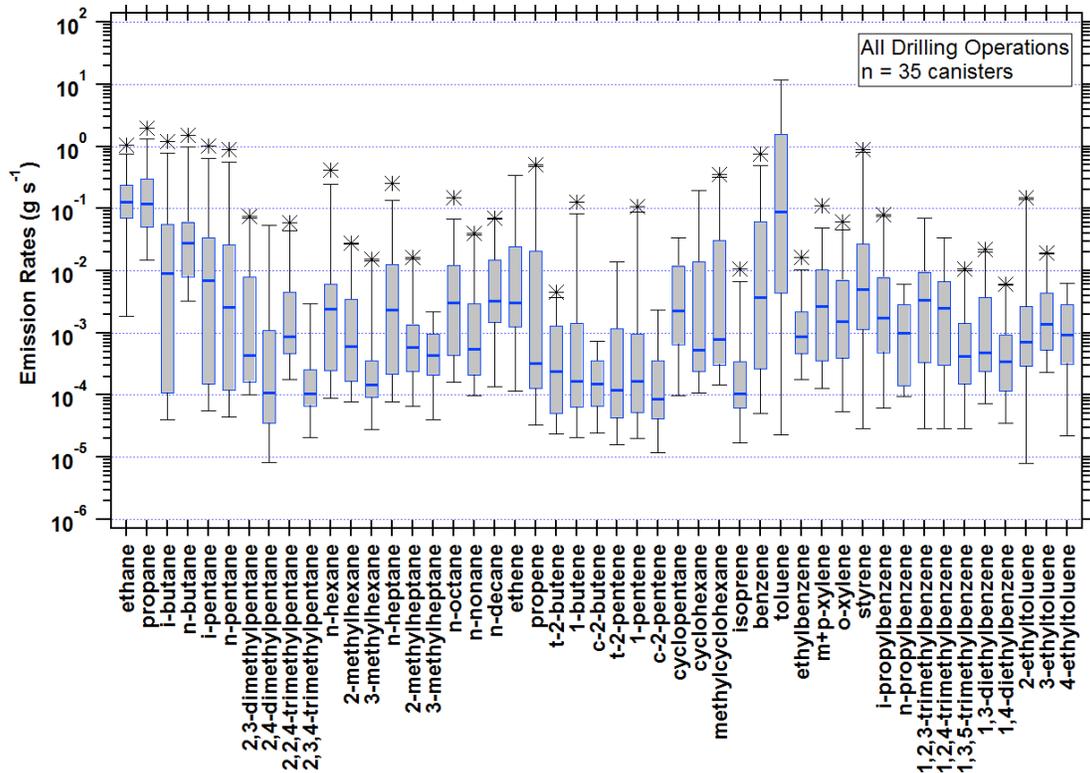

Figure 3.4. ERs of VOCs from canisters collected during drilling operations. The bottom and top of the boxes are the 25th and 75th percentiles, the blue line inside the box represents the median, the bottom and top whiskers are the 5th and 95th percentiles, and the stars are the outliers beyond the 5th and 95th percentiles. 35 canisters from 5 experiments are included in this figure.

Emissions during drilling operations are expected to reflect a mixture of combustion from engines and well emissions. This is reflected in the variability and trends observed in the VOC emissions. For example, the most abundant VOC emissions during drilling operations are seen for ethane and propane (important constituents of raw natural gas) and for toluene (a common component of engine exhaust emissions). Tabulated summaries of drilling operation ERs for several key VOCs, including average, median, and 25th and 75th percentiles are given in Table 3.3.

Table 3.3. Mean, median, 25th percentile and 75th percentile of the data for all canisters collected during drilling operations.

VOC	Mean (g s^{-1})	Median (g s^{-1})	25th %-ile (g s^{-1})	75th %-ile (g s^{-1})
Ethane	0.18	0.13	0.070	0.23
Propane	0.24	0.12	0.051	0.30
i-Pentane	0.079	0.0070	0.00015	0.034
n-Pentane	0.066	0.0026	0.00012	0.026
n-Decane	0.012	0.0033	0.0015	0.015
Ethene	0.040	0.0030	0.0012	0.024
Propene	0.042	0.00032	0.00013	0.021
Benzene	0.066	0.0037	0.00026	0.062
Toluene	1.48	0.088	0.0044	1.54
Ethylbenzene	0.0018	0.00086	0.00046	0.0022
m+p-Xylene	0.0095	0.0026	0.00035	0.010
o-Xylene	0.0085	0.0015	0.00040	0.0071

Figure 3.5 presents data from all fracking operations sampled during the study. Potential sources of emissions during fracking include combustion sources associated with power generation and any materials volatilized from chemicals used in fracking liquids. Direct emissions from the well are less likely during this operational stage when activity is pushing material into the wells. Consistent with these expectations, we see a relative increase in emission rates of aromatics and heavier alkanes (e.g., n-heptane, n-octane, n-nonane, benzene, and toluene) compared to the lighter alkanes (e.g., ethane and propane) typically associated with raw natural gas emissions. Tabulated summaries of fracking operation ERs for several key VOCs, including median and 25th and 75th percentiles are given in Table 3.4.

Table 3.4. Mean, median, 25th percentile and 75th percentile of the data for all canisters collected during fracking operations.

VOC	Mean (g s^{-1})	Median (g s^{-1})	25th %-ile (g s^{-1})	75th %-ile (g s^{-1})
Ethane	0.23	0.088	0.0035	0.31
Propane	0.032	0.013	0.0012	0.045
i-Pentane	0.022	0.00041	0.000052	0.011
n-Pentane	0.022	0.00027	0.000035	0.012
n-Decane	0.20	0.061	0.014	0.39
Ethene	0.025	0.0046	0.0013	0.025
Propene	0.011	0.0039	0.00056	0.011
Benzene	0.10	0.029	0.012	0.19
Toluene	0.51	0.12	0.050	0.89
Ethylbenzene	0.039	0.011	0.0049	0.076
m+p-Xylene	0.50	0.12	0.024	1.1
o-Xylene	0.086	0.021	0.0070	0.18

Figure 3.6 shows VOC ERs from all flowback operations. As expected, light alkane emissions are relatively abundant during this process, as emissions from flowback liquids emerging from the wells are likely to be important. Other important emissions included larger alkanes, toluene, and methylcyclohexane. Emissions of alkenes, which might be associated with combustion processes, were much lower. This is not surprising since combustion activities are generally limited on-site during flowback operations. Tabulated summaries of drilling operation ERs for several key VOCs, including median and 25th and 75th percentiles are given in Table 3.5.

Table 3.5. Mean, median, 25th percentile and 75th percentile of the data for all canisters collected during flowback operations.

VOC	Mean (g s^{-1})	Median (g s^{-1})	25th %-ile (g s^{-1})	75th %-ile (g s^{-1})
Ethane	3.9	0.93	0.27	5.4
Propane	1.5	0.37	0.11	2.0
i-Pentane	0.39	0.11	0.045	0.63
n-Pentane	0.31	0.081	0.034	0.52
n-Decane	0.25	0.11	0.050	0.29
Ethene	0.0095	0.0030	0.00076	0.0071
Propene	0.0030	0.00091	0.00030	0.0017
Benzene	0.094	0.062	0.020	0.12
Toluene	0.42	0.24	0.086	0.51
Ethylbenzene	0.043	0.017	0.0042	0.036
m+p-Xylene	0.25	0.16	0.047	0.35
o-Xylene	0.071	0.038	0.011	0.079

ERs from each experiment as described in Table 1.1 are presented in individual graphs and included as figures in Appendix D.
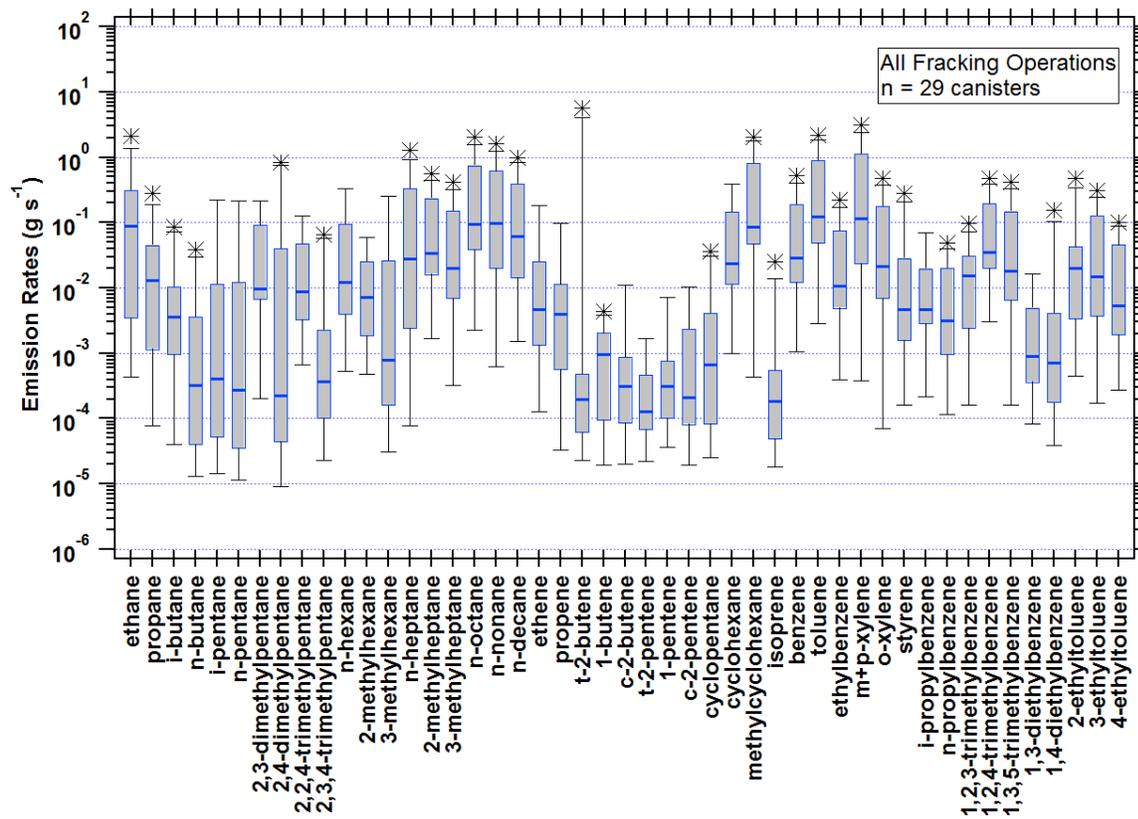
Figure 3.5. ERs of VOCs from canisters collected during fracking operations. The bottom and top of the boxes are the 25th and 75th percentiles, the blue line inside the box represents the median, the bottom and top whiskers are the 5th and 95th percentiles, and the stars are the outliers beyond the 5th and 95th percentiles. 29 canisters from 5 experiments are included in this figure.
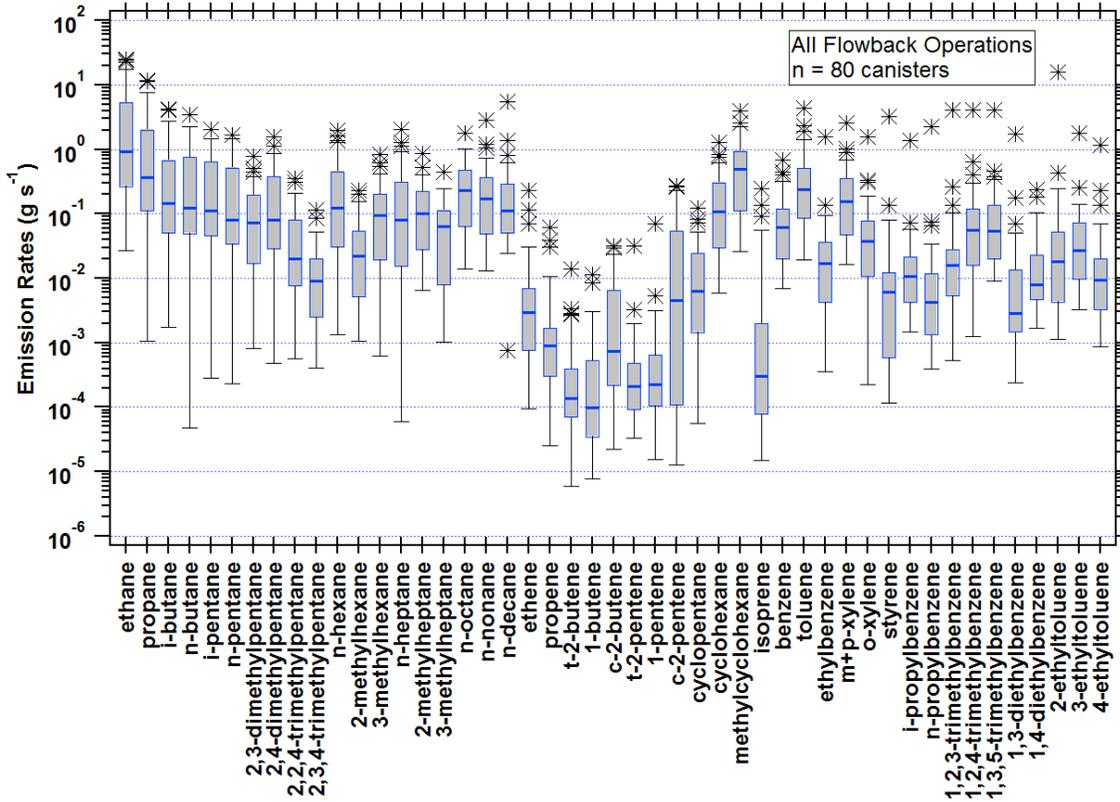
Figure 3.6. ERs of VOCs from canisters collected during flowback operations. The bottom and top of the boxes are the 25th and 75th percentiles, the blue line inside the box represents the median, the bottom and top whiskers are the 5th and 95th percentiles, and the stars are the outliers beyond the 5th and 95th percentiles. 80 canisters from 6 experiments are included in this figure.

In order to facilitate comparison of VOC ERs from different operation types, a subset of VOCs is chosen. Figure 3.7 summarizes ranges of ERs for the BTEX compounds. Median ERs of all BTEX compounds are highest for flowback and lowest for drilling, with fracking emissions intermediate. Figure 3.8 compares ER ranges for different operations for selected alkanes: ethane, propane, i-pentane, n-pentane, and n-decane. The flowback ERs for all of these compounds are typically higher than ERs from drilling or fracking. Median ERs of heavier alkanes from drilling are lower than those from fracking while the reverse is true for light alkanes.
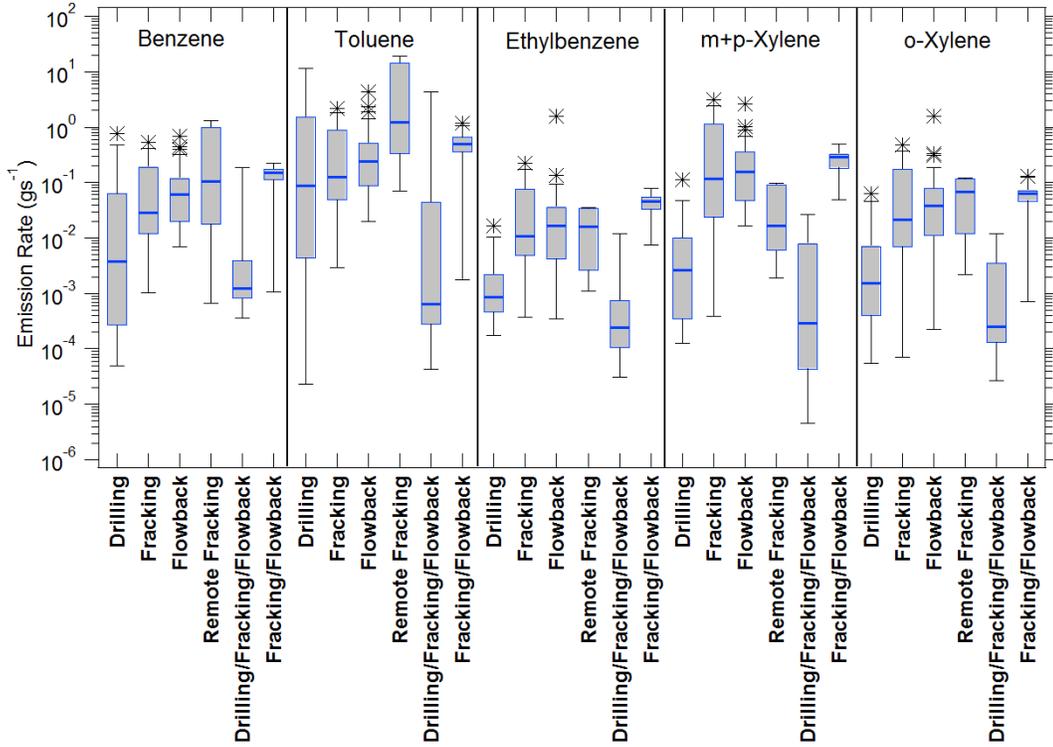
Figure 3.7. Ranges of ERs of BTEX for different operation types. The bottom and top of the boxes are the 25th and 75th percentiles, the blue line inside the box represents the median, the bottom and top whiskers are the 5th and 95th percentiles, and the stars are the outliers beyond the 5th and 95th percentiles.
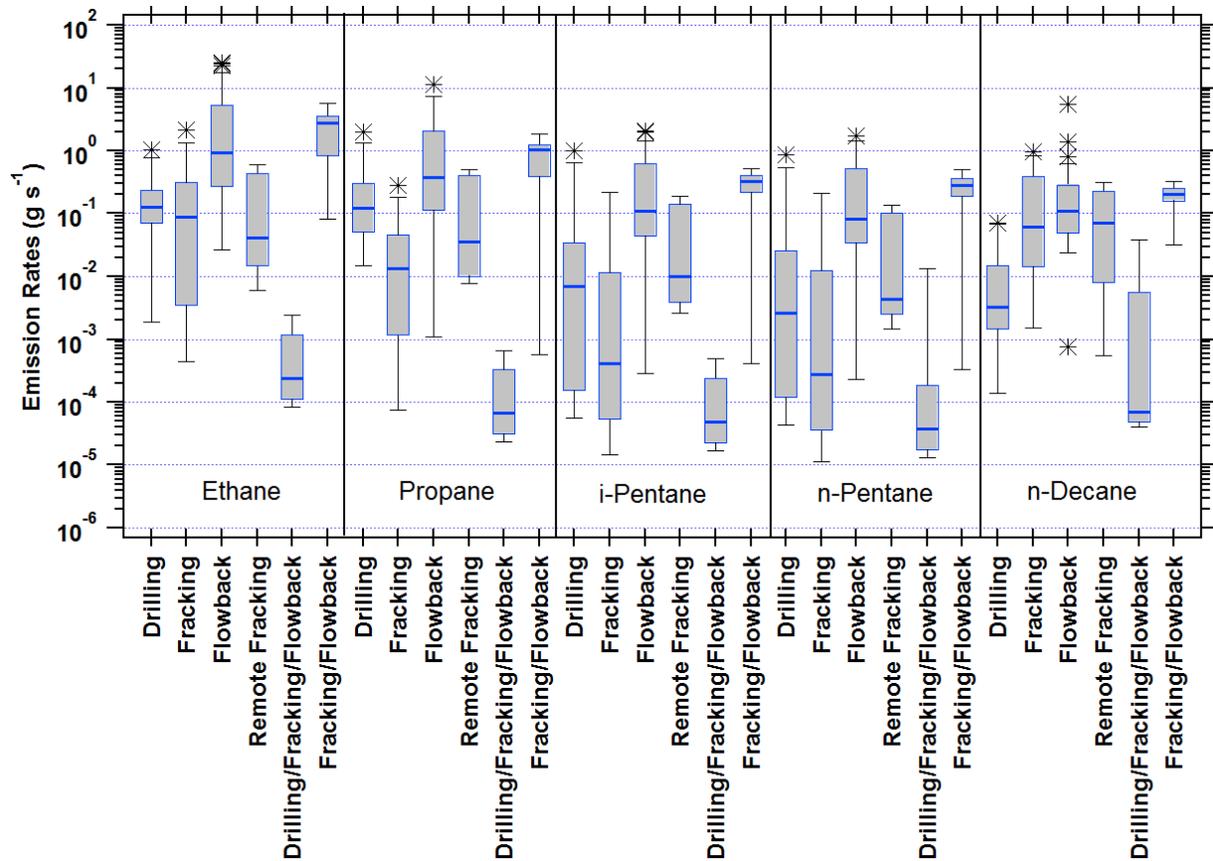
Figure 3.8. Ranges of ERs for selected alkanes for different operation types. The bottom and top of the boxes are the 25th and 75th percentiles, the blue line inside the box represents the median, the bottom and top whiskers are the 5th and 95th percentiles, and the stars are the outliers beyond the 5th and 95th percentiles.

3.3.   Dispersion Modeling

3.3.1.   AERMOD Replication of Field Measurements

AERMOD was used to model the downwind concentrations for several emission experiments conducted during the study. Local observations from the meteorological station and larger scale reanalysis data concerning atmospheric boundary layer properties were used as input to AERMOD. The dispersion of the tracer, acetylene, was simulated in the model because it was the gas where both the release rate and location were most accurately known. For this comparison, the model receptors were placed exactly at the locations of the collection of canisters (vertically and horizontally). The background-corrected concentration of acetylene in each canister was compared to the hourly averaged concentrations predicted by AERMOD and the results are presented in Figure 3.9.
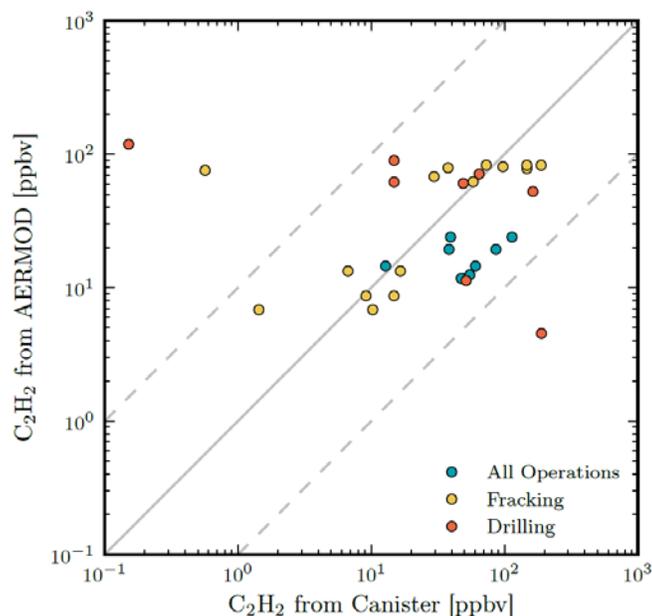
Figure 3.9. Comparison of canister acetylene concentration measurements to AERMOD estimates. The gray line represents the 1:1 line. The dashed gray lines encompass 28 out of 31 points, within a factor of 10 of the 1:1 line.

In general, AERMOD was able to predict concentrations with a small overall bias but with a moderate degree of scatter. The model and measurement comparison had a correlation coefficient of 0.0014, the log mean bias of this comparison is -0.13, and the slope is 0.74. 28 out of 31 points are located within a factor of 10 of the 1:1 line. However, there are 2 high and 1 low outliers in Figure 3.9 that fall outside of a factor of 10 of the 1:1 line. Some outliers may reflect AERMOD's incorrect representation of atmospheric instability which may have resulted in insufficient or excess dilution of acetylene in the plume. Misalignment of the modeled and actual plumes could also be an issue; even small differences in the direction of plume advection in AERMOD could yield a significant difference between modeled and observed concentrations of highly transient plumes. It is important to note that canisters were sampled for three minutes and AERMOD concentration fields were resolved to one hour intervals, which makes a prediction between simulated and observed values especially challenging. Sampling times less than 10-20 minutes may have winds dominated by turbulent eddies rather than the mean wind under unstable atmospheric conditions.

3.3.2. The Use of Dispersion Modeling Under Various Meteorological Conditions to Translate Study Emission Rates to Concentration Fields

The primary focus of this study was to determine activity-specific air pollutant emission rates, and their variability, for a range of compounds of interest, including methane and several VOCs. Such emissions information is very useful for predicting concentration fields of similar operations for locations and times of interest, where topography and meteorological conditions might differ substantially from the conditions studied here. Concentration field predictions of this type, for example, would provide useful input for future health risk assessments attempting to quantify effects of exposure to emissions from gas well drilling and completions. Emission rates from this study, for example, can be used along with meteorological conditions and topography for any time period and location of interest to drive AERMOD predictions of temporal and spatial concentration fields.

To illustrate such an approach, the 2014 North American Regional Reanalysis (NARR) dataset with meteorological values taken from a region in Garfield County, CO were used to simulate the concentration field for a typical site with benzene emitted at a rate of 0.23 g s^{-1} under different meteorological conditions. Figure 3.10 shows the simulated seasonal mean benzene concentration fields. It is important to note that this sample analysis assumes that benzene was emitted at a constant rate throughout the simulation in order to better represent the average seasonal concentration fields expected across varying weather conditions. The 0.23 g s^{-1} emission rate chosen here is among the larger values observed during the study, exceeding the 75th percentile values observed for drilling, fracking, and flowback. One can scale the benzene concentration field for other emission rates by multiplying the modeled concentration at any point by the ratio of the new emission rate divided by 0.23 g s^{-1}.
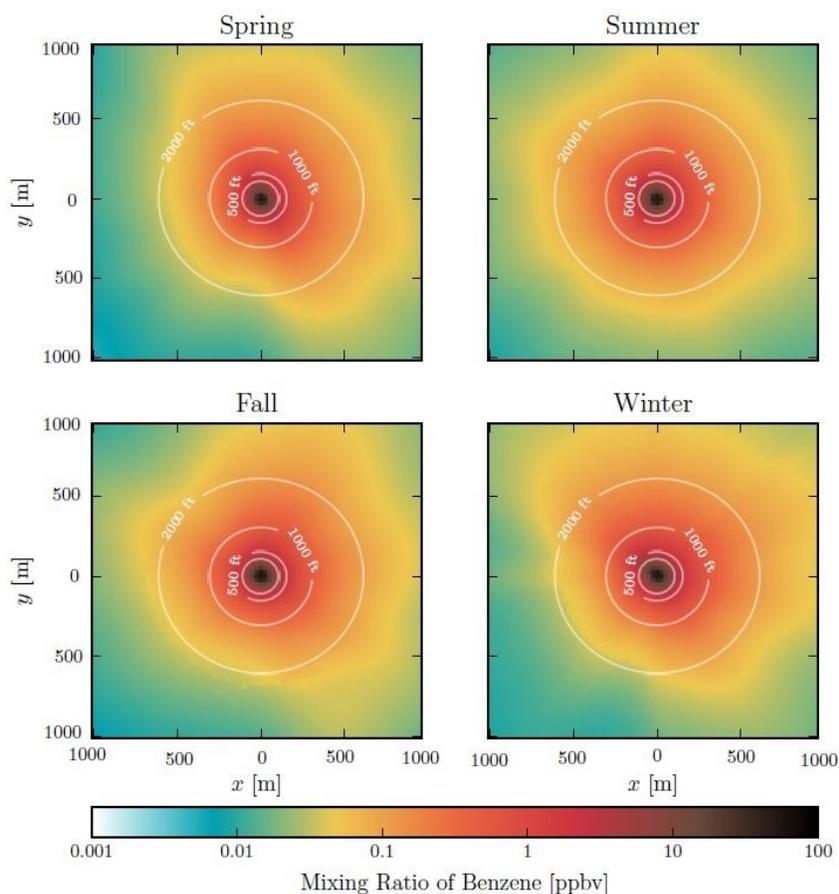
Figure 3.10. The mean benzene seasonal concentration fields predicted by AERMOD at a typical site in western Colorado using a constant benzene ER of 0.23 g s^{-1}. This emission rate is among the upper end of emission values measured during this study.

The well pad emissions location in the figure is positioned at (x; y) = (0 m; 0 m) and the model was simulated with a horizontal resolution of 25 m. The colors represent the seasonal average concentration of benzene surrounding the site. The color bar uses a log-scale due to the concentrations spanning three orders of magnitude over the 4 km^2 domain. The seasonal mean concentrations are somewhat evenly distributed radially surrounding the well pad. Some preference toward higher concentrations north and east of the pad reflect a predominance of wind transport towards those directions in the 2014 seasonal meteorology. The differences in the concentration fields across the four seasons are relatively small,

suggesting that emission impacts upon the area surrounding the wellpad are likely to be similar, on average, for different times of year. Extended and/or more complex simulations of this type are, of course, also possible. For example: (1) one could conduct similar simulations for other VOCs of interest, (2) one could vary emissions rates (e.g., over time) to reflect the range of emission rates observed for compounds of interest in this study and look at impacts on predicted concentration fields, (3) one could examine composite concentration fields resulting from emissions at multiple well locations in a region of interest, and (4) one could look at the probability of exposure to a range of VOC concentration levels of interest as a function of a particular location or at a particular distance of interest.

4. References

Cimorelli, A. J., S. G. Perry, R. F. Lee, R. J. Paine, A. Venkatram, J. C. Weil, and R. B. Wilson, (1996) Current Progress in the AERMIC Model Development Program. Preprints, 89th Annual Meeting Air and Waste Management Association, Air and Waste Management Association, Pittsburgh, PA.

Galle, B., J. Samuelsson, B. H. Svensson, and G. Börjesson, (2000) Measurements of Methane Emissions from Landfills Using a Time Correlation Tracer Method Based on FTIR Absorption Spectroscopy, Environ. Sci. Tech., 35 (1), pp. 21-25, doi:10.1021/es0011008.

Johnson, R. C., J. E. Birdwell, T. J. Mercier, and M. E. Brownfield, (2016) Geology of Tight Oil and Potential Tight Oil Reservoirs in the Lower Part of the Green River Formation, Uinta, Piceance, and Greater Green River Basins, Utah, Colorado, and Wyoming: U.S. Geological Survey Scientific Investigations Report 2016-5008, doi:10.3133/sir20165008.

Kaharabata, S. K., and P. H. Schuepp, (2000) Estimating Methane Emissions from Dairy Cattle Housed in a Barn and Feedlot Using an Atmospheric Tracer, Environ. Sci. Tech., 34 (15), pp. 3296-3302, doi:10.1021/es990578c.

Lamb, B. K., H. Westberg, and G. Allwine, (1986) Isoprene Emission Fluxes Determined by an Atmospheric Tracer Ratio Technique, Atmos. Environ., 30 (24), 4209-4223, doi:10.1016/0004-6981(86)90201-5.

Lamb, B. K., J. B. McManus, J. H. Shorter, C. E. Kolb, B. Mosher, R. C. Harriss, E. Allwine, D. Blaha, T. Howard, A. Guenter, R. A. Lott, R. Siverson, H. Westburg, and P. Zimmerman, (1995) Development of Atmospheric Tracer Methods to Measure Methane Emissions from Natural Gas Facilities and Urban Areas, Environ. Sci. Technol, 29 (6), pp. 1468-1479, doi:10.1021/es00006a007.

Lassey, K. R., M. J. Ulyatt, R. J. Martin, C. F. Walker, and I.D. Shelton, (1997) Methane Emissions Measured Directly from Grazing Livestock in New Zealand, Atmos. Environ., 31 (18), pp. 2905-2914, doi:10.1016/S1352-2310(97)001234.

MacDonald, L., (2015) Estimating Emission Rates of Volatile Organic Compounds from Oil and Natural Gas Operations in the Piceance Basin, M.S. thesis, Colorado State Univ., Fort Collins, CO, Fall.

Mønster, J. G., J. Samuelsson, P. Kjeldsen, C. W. Rella, and C. Scheutz, (2014) Quantifying Methane Emission from Fugitive Sources by Combining Tracer Release and Downwind Measurements – A Sensitivity Analysis Based on Multiple Field Surveys, Waste Manag., 34 (8), pp. 1416-1428, doi:10.1016/j.wasman.2014.03.025.

Rumburg, B., G. H. Mount, J. Filipy, B. Lamb, H. Westberg, D. Yonge, R. Kincaid, and K. Johnson, (2008) Measurement and Modeling of Atmospheric Flux of Ammonia from Dairy Milking Cow Housing, Atmos. Environ., 42 (14), pp. 3364-3379, doi:10.1016/j.atmosenv.2007.05.042.

Scholtens, R., C. J. Dore, B. M. R. Jones, D. S. Lee, and V. R. Phillips, (2004) Measuring Ammonia Emission Rates from Livestock Buildings and Manure Stores – Part 1: Development and Validation of External Tracer Ratio, Internal Tracer Ratio and Passive Flux Sampling Methods, Atmos. Environ., 38 (19), pp. 3003-3015, doi:10.1016/j.atmosenv.2004.02.030.

Swarthout, R. F., (2014) Volatile Organic Compound Emissions from Unconventional Natural Gas Production: Source Signatures and Air Quality Impacts, Ph.D. Dissertation, Univ. of New Hampshire, Durham, NH, May.

Wells, B., (2015) The Validation of Emission Rate Estimation Methods, M.S. thesis, Colorado State Univ., Fort Collins, CO, Spring.

Wells, B. L., L. P. Macdonald, K. Shonkwiler, A. Clements, A. Hecobian, J. Ham, J. R. Pierce, and J. L. Collett, Jr., (2016) Estimating Hydrocarbon Emissions Using Stationary Tracer Techniques, Manuscript in preparation.

Appendix A

Background Canister Concentration Statistics

During each experiment 1-2 canisters were collected upwind of the measurement site to evaluate the effect of regional air and other sources on VOCs. The mean, median, and standard deviations of all canisters collected to represent background VOC concentrations during this study are presented in Table A.1.

Table A.1. Mean, median, and standard deviation of background VOC concentrations for background samples collected at all sites. All units are in ppbv.

VOC (ppbv)	Mean (ppbv)	Median (ppbv)	Standard Deviation (ppbv)
ethane	12.83	6.77	14.89
ethene	0.76	0.46	0.89
propane	14.71	3.32	41.17
propene	0.16	0.07	0.18
i-butane	3.28	1.06	7.39
n-butane	5.91	1.06	17.95
acetylene	0.72	0.32	0.89
t-2-butene	0.02	0.01	0.03
1-butene	0.06	0.04	0.07
c-2-butene	0.06	0.02	0.11
cyclopentane	0.14	0.03	0.33
i-pentane	2.23	0.64	4.84
n-pentane	2.18	0.44	5.62
t-2-pentene	0.02	0.01	0.04
1-pentene	0.03	0.01	0.04
c-2-pentene	0.07	0.02	0.09
n-hexane	0.66	0.22	1.68
isoprene	0.06	0.01	0.13
2,4-dimethylpentane	0.12	0.06	0.14
n-heptane	0.30	0.12	0.61
benzene	0.58	0.27	0.61
cyclohexane	0.37	0.16	0.61
2,3-dimethylpentane	0.16	0.07	0.33
2-methylhexane	0.07	0.03	0.10
3-methylhexane	0.12	0.04	0.16
2,2,4-trimethylpentane	0.24	0.06	0.74
methylcyclohexane	0.29	0.21	0.27
2,3,4-trimethylpentane	0.01	0.00	0.02
toluene	4.70	0.46	10.87
2-methylheptane	0.13	0.06	0.21
3-methylheptane	0.12	0.07	0.13
ethylbenzene	0.06	0.03	0.05
n-octane	0.22	0.15	0.33

VOC (cont.) (ppbv)	Mean (ppbv)	Median (ppbv)	Standard Deviation (ppbv)
m+p-xylene	0.16	0.14	0.11
styrene	0.12	0.10	0.10
o-xylene	0.11	0.08	0.09
n-nonane	0.13	0.08	0.11
i-propylbenzene	0.02	0.01	0.03
n-propylbenzene	0.01	0.01	0.02
3-ethyltoluene	0.04	0.02	0.03
4-ethyltoluene	0.02	0.01	0.01
1,3,5-trimethylbenzene	0.06	0.04	0.05
1,4-diethylbenzene	0.37	0.16	0.87

Appendix B

GC Systems Calibration Statistics

Table B.1 contains calibration statistics for the VOCs measured on the multi-channel system and Table B.2 contains calibration statistics for the VOCs measured on the HP GC-FID system.

Table B.1. Calibration statistics for VOCs measured using the multi-channel GC system.

VOC	Calibration r²	LOD (ppbv)	Slope of the Calibration Curve (peak area/ppbv)	Standard Range (ppbv)
ethane	0.999	0.105	137	0.4-3362
propane	0.999	0.020	1294	0.4-3203
i-butane	0.999	0.008	1682	0.4-3171
n-butane	0.999	0.010	1691	0.4-3140
cyclopentane	0.999	0.009	2097	0.4-3171
i-pentane	0.999	0.009	2110	0.4-3171
n-pentane	0.998	0.007	2039	0.4-3108
2,4-dimethylpentane	0.992	0.004	4049	0.4-3330
2,3-dimethylpentane	0.998	0.013	1049	0.4-3362
2,2,4-trimethylpentane	0.998	0.018	1196	0.4-3298
2,3,4-trimethylpentane	0.999	0.009	1174	0.4-3299
n-hexane	0.999	0.012	2467	0.4-3267
2-methylhexane	0.999	0.010	1079	0.4-3299
3-methylhexane	0.999	0.014	1064	0.4-3299
n-heptane	0.995	0.009	3164	0.4-3299
2-methylheptane	0.999	0.022	1165	0.4-3299
3-methylheptane	0.999	0.016	1177	0.4-3267
n-octane	0.999	0.016	1115	0.4-3299
n-nonane	0.999	0.010	1165	0.4-3235
n-decane	0.999	0.011	1131	0.4-3299
cyclohexane	0.999	0.015	895	0.4-3330
methylcyclohexane	0.999	0.019	1058	0.4-3299

VOC (cont.)	Calibration r²	LOD (ppbv)	Slope of the Calibration Curve (peak area/ppbv)	Standard Range (ppbv)
Ethene	0.999	0.053	945	0.4-3362
propene	0.999	0.009	1179	0.4-3203
t-2-butene	0.999	0.018	1662	0.4-3108
1-butene	0.998	0.013	1651	0.4-3104
c-2-butene	0.999	0.022	1756	0.4-3362
isoprene	0.998	0.012	2202	0.4-3171
t-2-pentene	0.996	0.014	1809	0.4-3203
1-pentene	0.998	0.023	1909	0.4-3076
c-2-pentene	0.998	0.012	1917	0.4-3330
benzene	0.999	0.010	903	0.4-3266
1,3,5-trimethylbenzene	0.999	0.012	1091	0.4-3235
1,2,3-trimethylbenzene	0.996	0.012	1074	0.4-3140
1,2,4-trimethylbenzene	0.997	0.0124	1077	0.4-3171
ethylbenzene	0.999	0.019	1066	0.4-3266
1,3-diethylbenzene	0.998	0.027	1136	0.4-3140
1,4-diethylbenzene	0.998	0.013	1133	0.4-3108
i-propylbenzene	0.999	0.011	1171	0.4-3140
n-propylbenzene	0.998	0.012	1157	0.4-3108
toluene	0.998	0.017	1028	0.4-3266
2-ethyltoluene	0.999	0.025	1128	0.4-3140
3-ethyltoluene	0.995	0.014	1084	0.4-3235
4-ethyltoluene	0.998	0.015	1102	0.4-3171
styrene	0.996	0.014	1008	0.4-3298
m+p-xylene	0.995	0.014	1754	0.4-3298
o-xylene	0.999	0.006	1087	0.4-3203
acetylene	0.999	0.013	1186	0.4-3362

Table B.2. Calibration statistics for VOCs measured using the HP GC-FID system.

VOC	Calibration r^2	LOD (ppbv)	Slope of Calibration Curve (peak area/ppbv)	Standard Range (ppbv)
ethane	0.904	0.073	3493	0.1 - 1000
propane	0.999	0.069	10539	0.1 - 1000
i-butane	0.999	0.047	13871	0.1 - 1000
n-butane	0.999	0.049	13854	0.1 - 1000
cyclopentane	0.999	0.024	14406	0.1 - 1000
i-pentane	0.999	0.014	17651	0.1 - 1000
n-pentane	0.999	0.017	17411	0.1 - 1000
2,4-dimedimethylpentane	0.999	0.245	21116	0.1 - 1000
2,2,4-trimethylpentane	0.995	0.004	60829	0.1 - 1000
n-hexane	0.999	0.014	45754	0.1 - 1000
n-heptane	0.999	0.003	27050	0.1 - 1000
n-octane	0.997	0.012	35396	0.1 - 1000
cyclohexane	0.998	0.012	22689	0.1 - 1000
ethene	0.990	0.069	3393	0.1 - 1000
propene	0.999	0.012	19815	0.1 - 1000
t-2-butene	0.999	0.033	13459	0.1 - 1000
i-butene	0.999	0.022	17959	0.1 - 1000
isoprene	0.996	0.035	6705	0.1 - 1000
t-2-pentene	0.963	0.091	3446	0.1 - 1000
1-pentene	0.999	0.019	16456	0.1 - 1000
cis-2-pentene	0.978	0.015	22972	0.1 - 1000
benzene	0.999	0.009	54563	0.1 - 1000
ethylbenzene	0.998	0.011	31507	0.1 - 1000
toluene	0.997	0.015	26110	0.1 - 1000
m+p-xylene	0.997	0.009	62256	0.1 - 1000
o-xylene	0.999	0.009	31822	0.1 - 1000
acetylene	0.947	0.092	7022	0.1 - 1000

Appendix C

Real-time Methane ERs for Several Experiments

Figures C.1 to C.16 show the normalized frequency distribution of real-time methane ERs for experiments where the data satisfied the conditions set in Section 2.3.1. Some experiments (Figures C.2 and C.6) contain data from more than one experiment. T is the number of hours of data available. Data were collected at 3Hz.
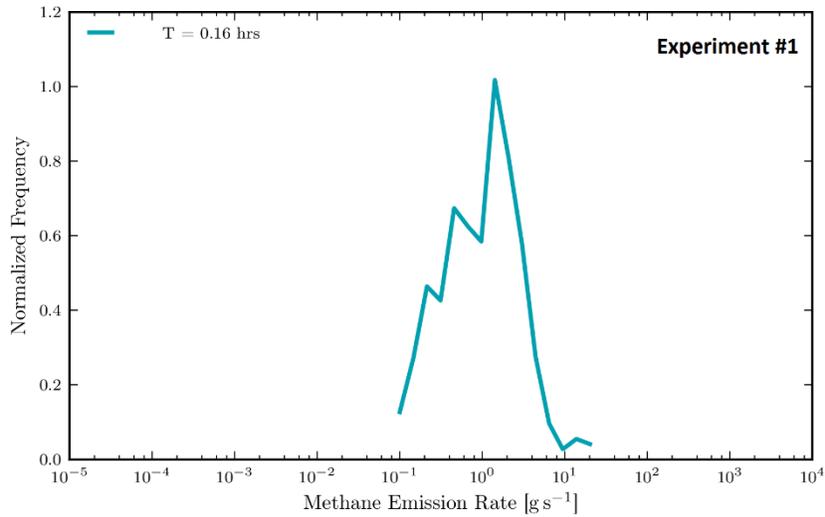
Figure C.1. Methane ER normalized frequency distributions from Experiment #1.
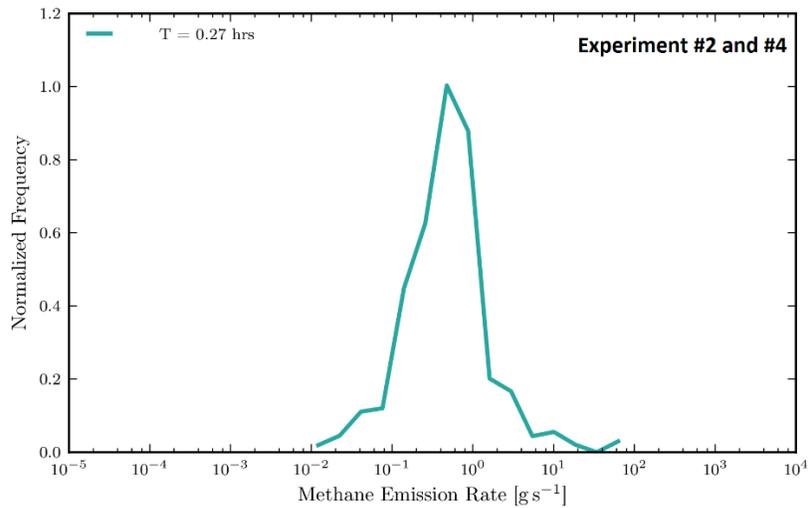
Figure C.2. Methane ER normalized frequency distributions from Experiments #2 and #4.
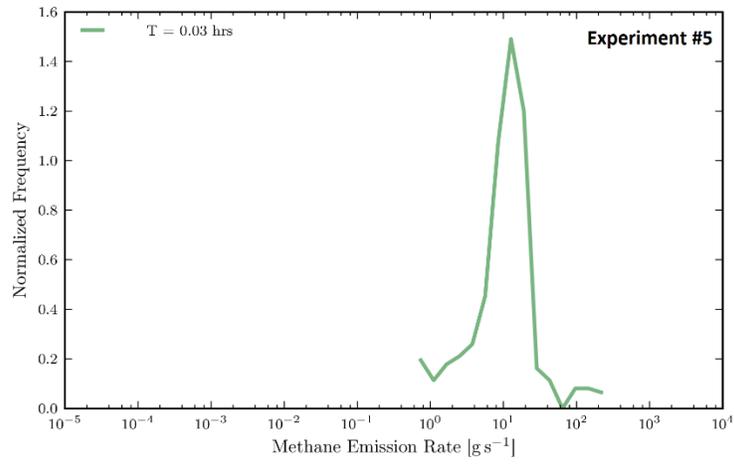
Figure C.3. Methane ER normalized frequency distributions from Experiment #5.
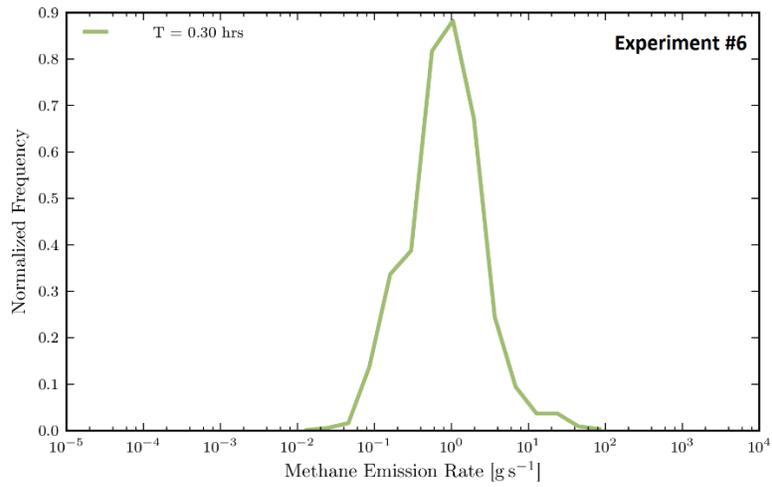
Figure C.4. Methane ER normalized frequency distributions from Experiment #6.
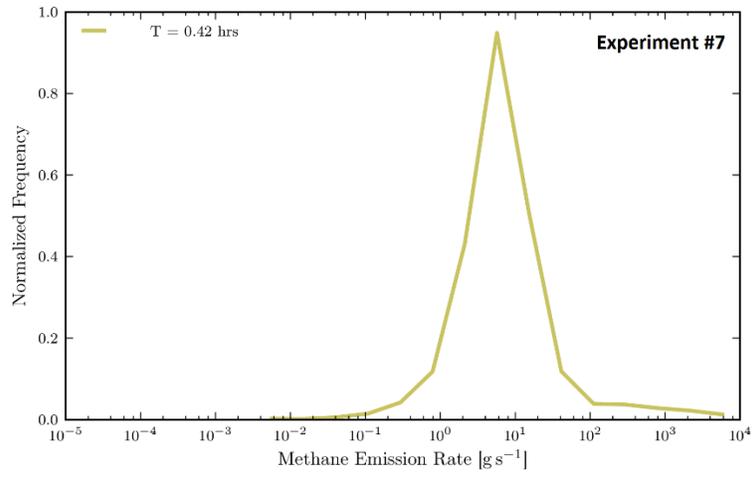
Figure C.5. Methane ER normalized frequency distributions from Experiment #7.
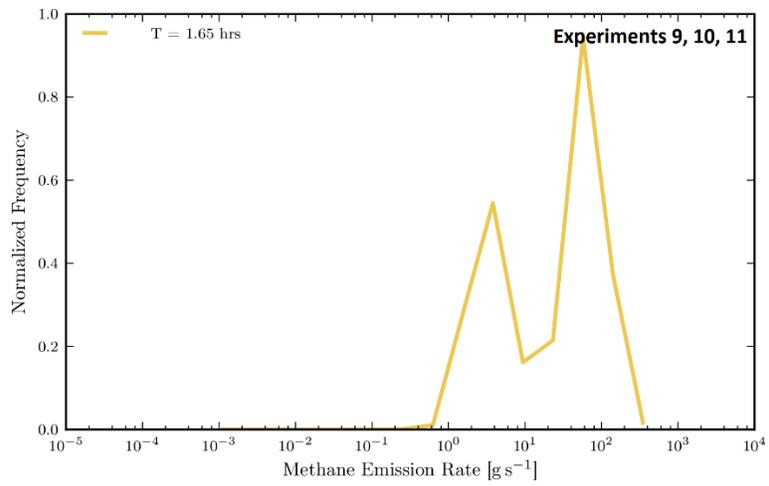
Figure C.6. Methane ER normalized frequency distributions from Experiment #9, 10, and 11.
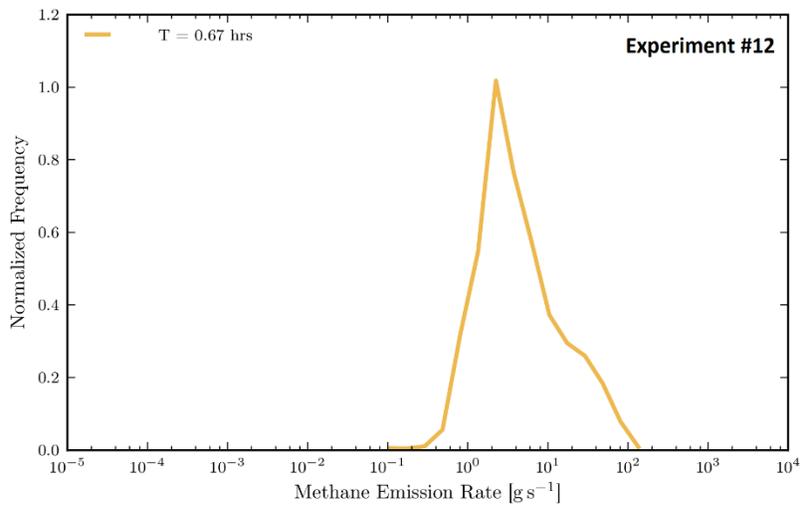
Figure C.7. Methane ER normalized frequency distributions from Experiment #12.
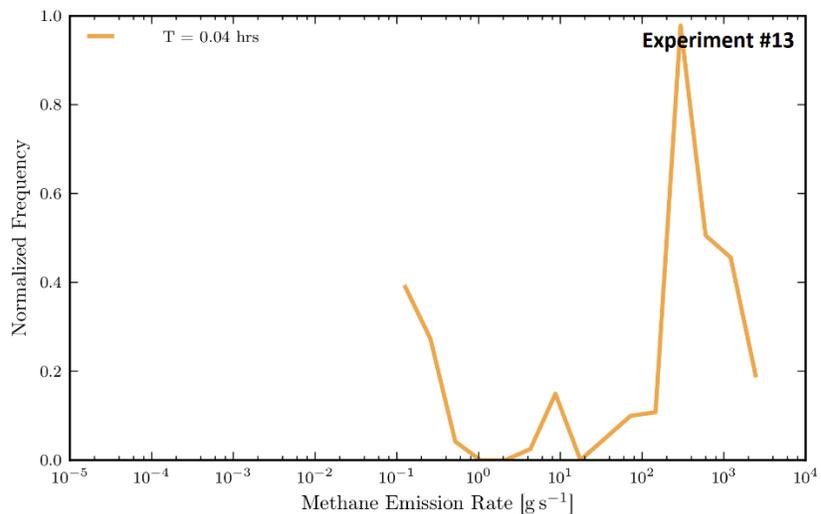
Figure C.8. Methane ER normalized frequency distributions from Experiment #13.
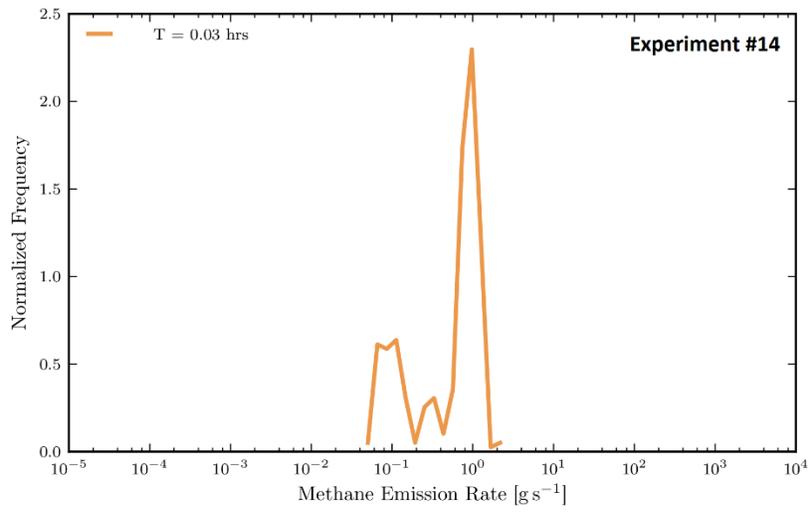
Figure C.9. Methane ER normalized frequency distributions from Experiment #14.
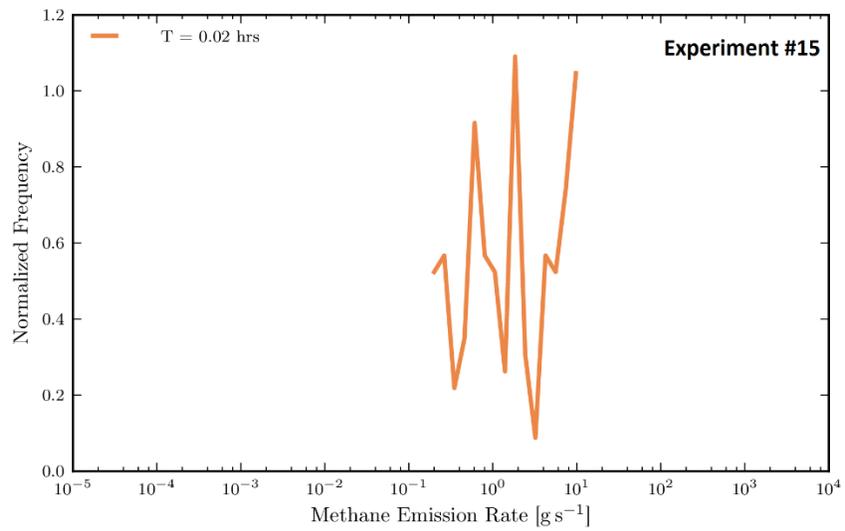
Figure C.10. Methane ER normalized frequency distributions from Experiment #15.
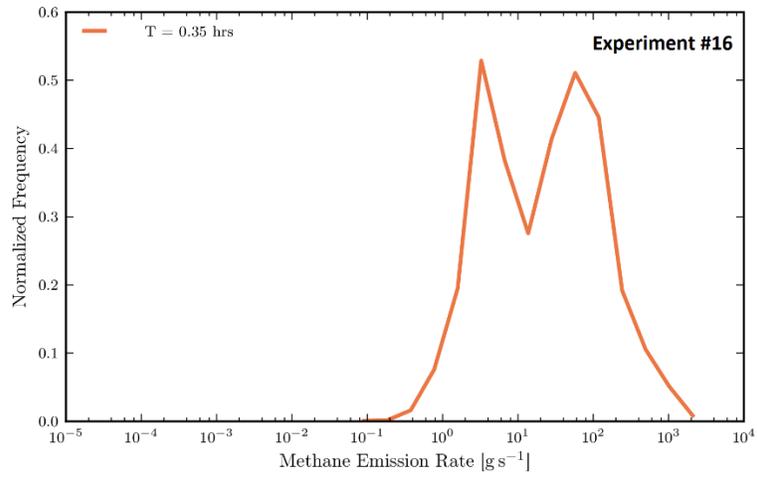
Figure C.11. Methane ER normalized frequency distributions from Experiment #16.
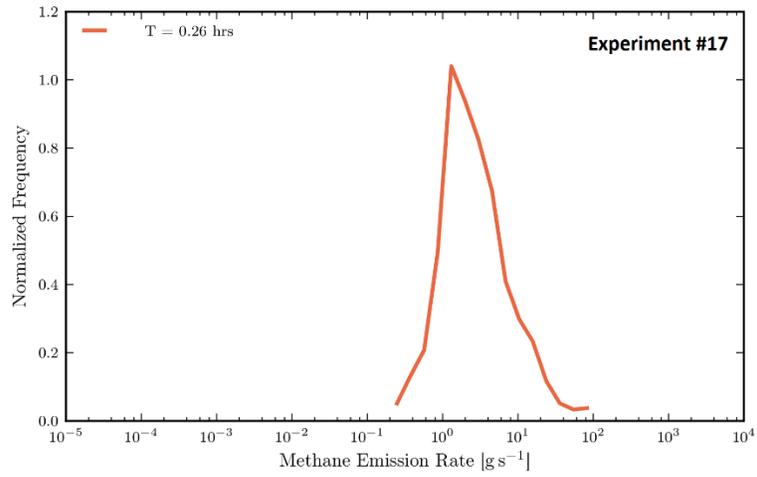
Figure C.12. Methane ER normalized frequency distributions from Experiment #17.
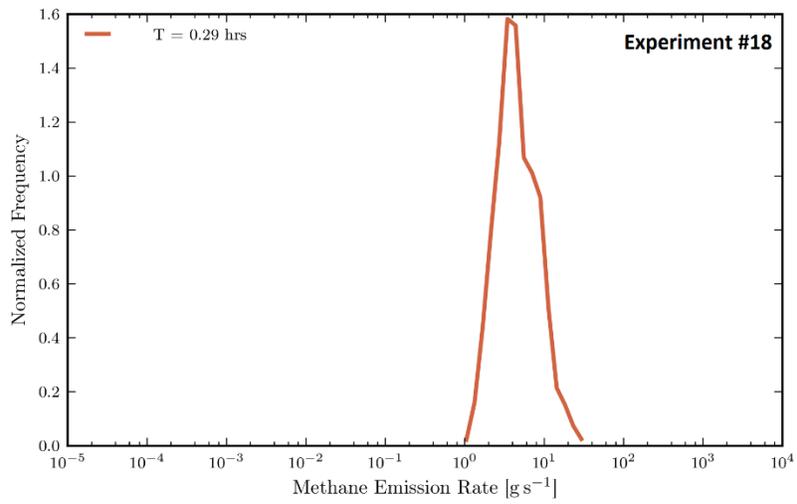
Figure C.13. Methane ER normalized frequency distributions from Experiment #18.
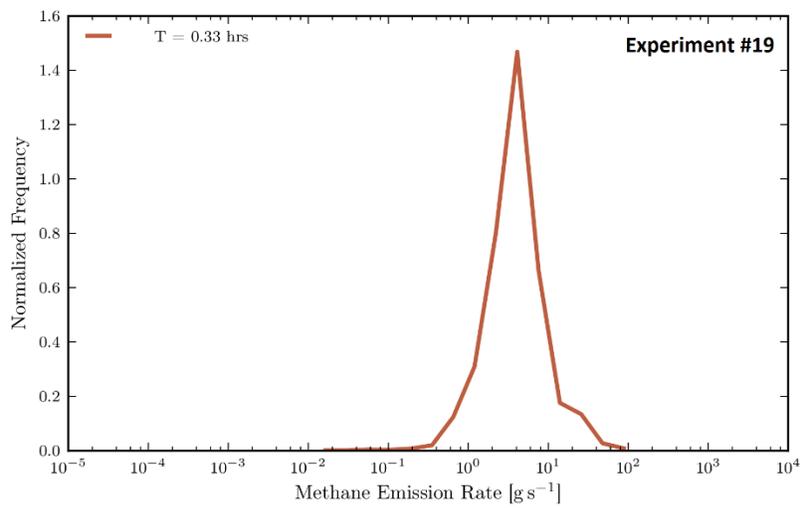
Figure C.14. Methane ER normalized frequency distributions from Experiment #19.
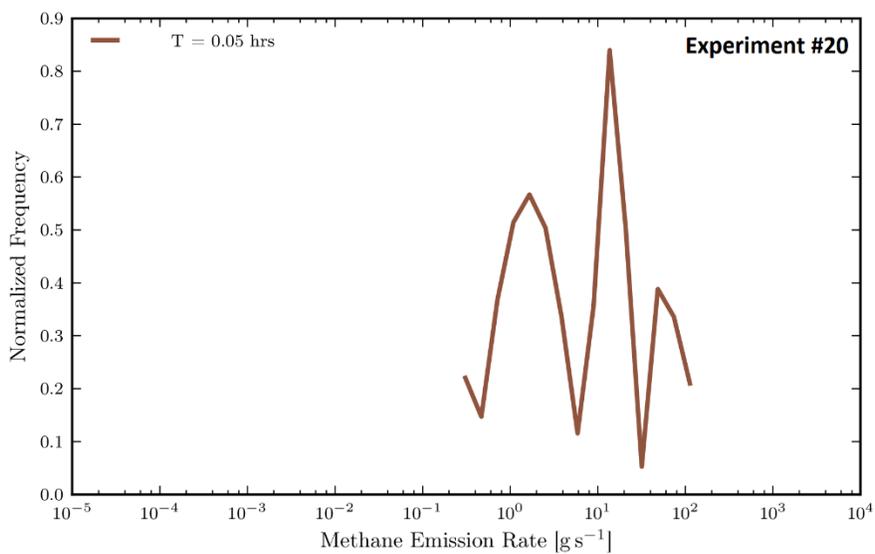
Figure C.15. Methane ER normalized frequency distributions from Experiment #20.
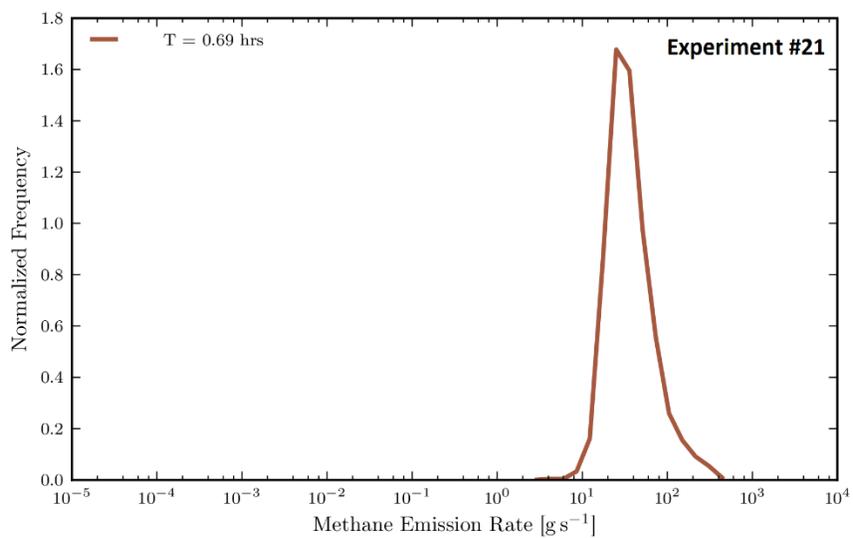
Figure C.16. Methane ER normalized frequency distributions from Experiment #21.

Appendix D

ERs of VOCs from Individual Experiments

The following figures present ERs of VOCs from individual experiments. Figures D.1 and D.2 contain VOCs analyzed using the HP GC-FID system, Figures D.3 to D.20 present VOC ER results from canisters that were analyzed using the multi-channel GC-FID system. No canisters from experiment 3 are presented as none passed the criteria outlined in Section 2.3.2.
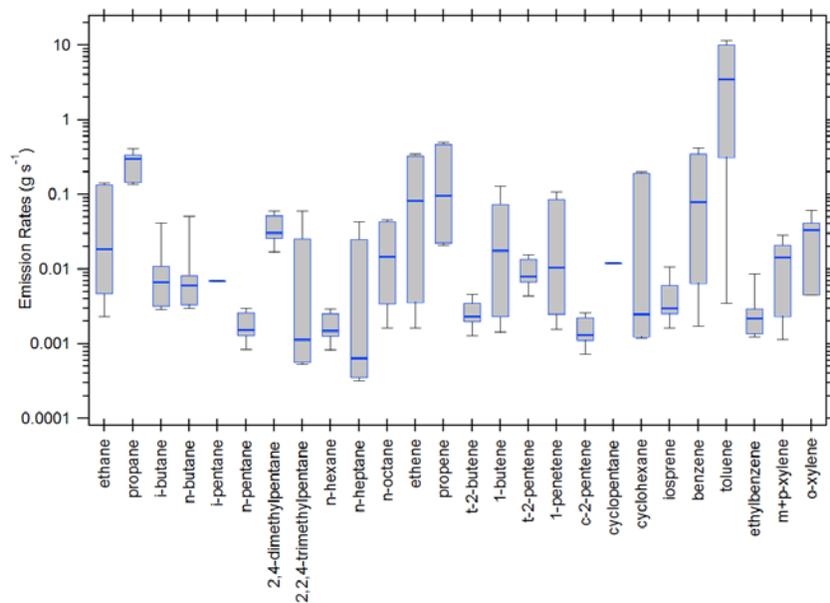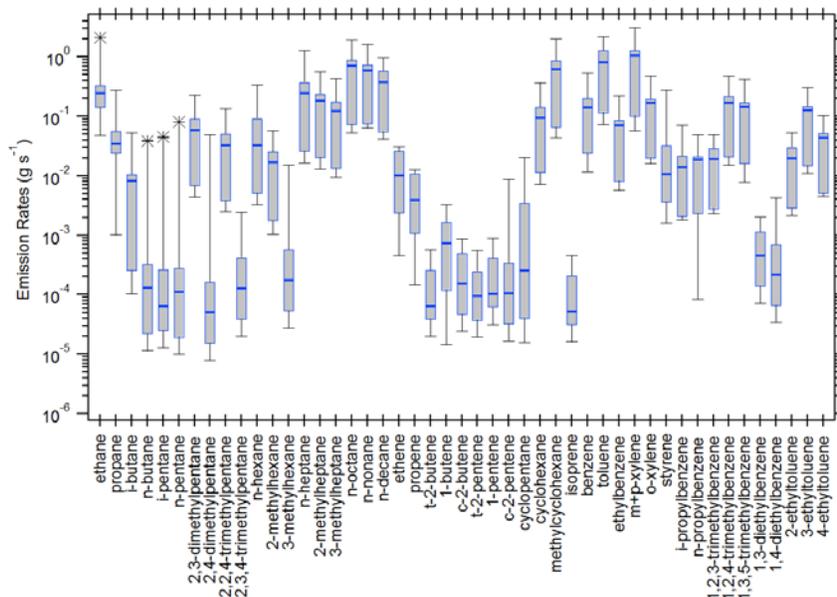

Figure D.1. ERs of VOCs from canisters collected during experiment #1 (drilling; n=13 canisters). The bottom and top of the boxes are the 25th and 75th percentiles, the blue line inside the box represents the median, the bottom and top whiskers are the 5th and 95th percentiles.
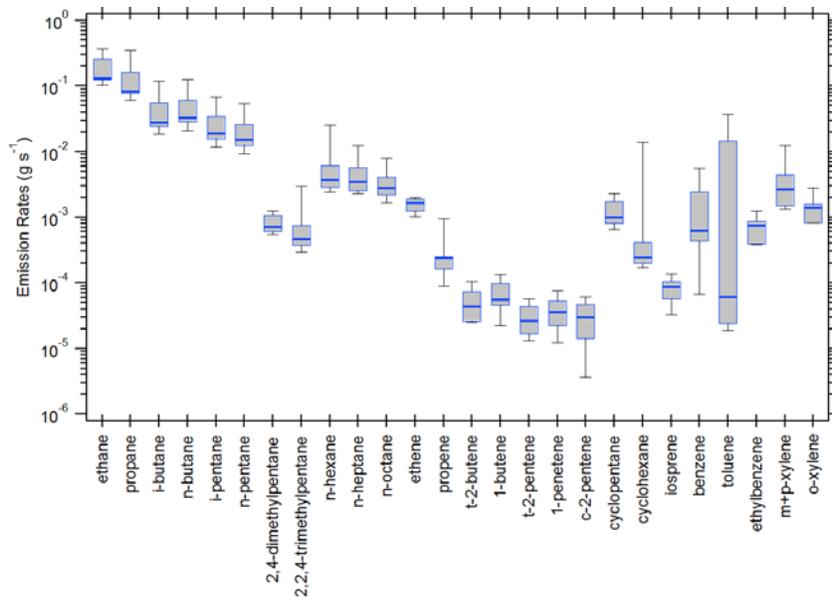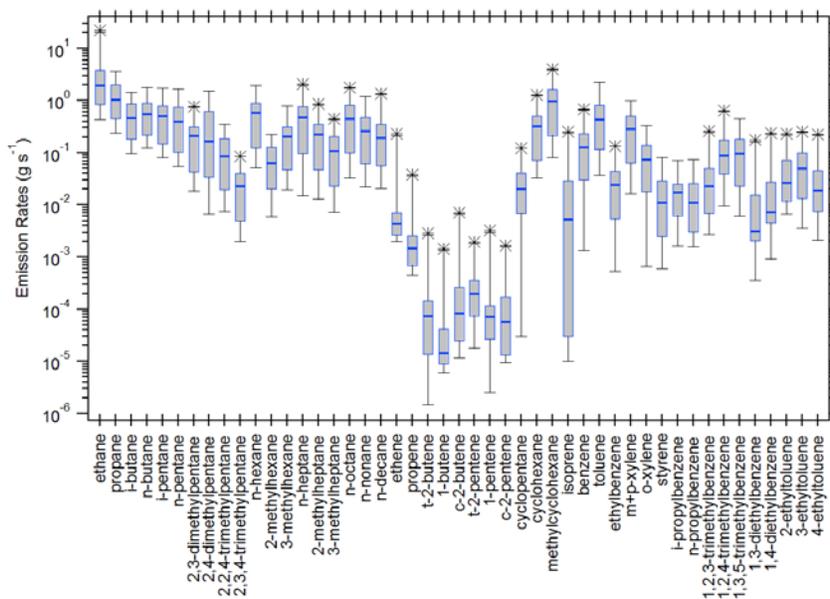
Figure D.2. ERs of VOCs from canisters collected during experiment #2 (drilling; n=16 canisters). The bottom and top of the boxes are the 25th and 75th percentiles, the blue line inside the box represents the median, the bottom and top whiskers are the 5th and 95th percentiles.
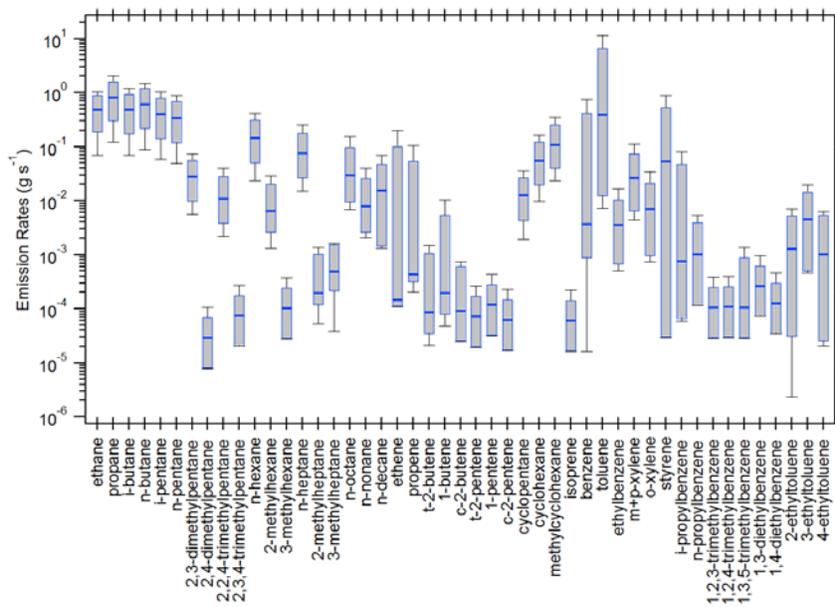
Figure D.3. ERs of VOCs from canisters collected during experiment #4 (drilling; n=6 canisters). The bottom and top of the boxes are the 25th and 75th percentiles, the blue line inside the box represents the median, the bottom and top whiskers are the 5th and 95th percentiles.
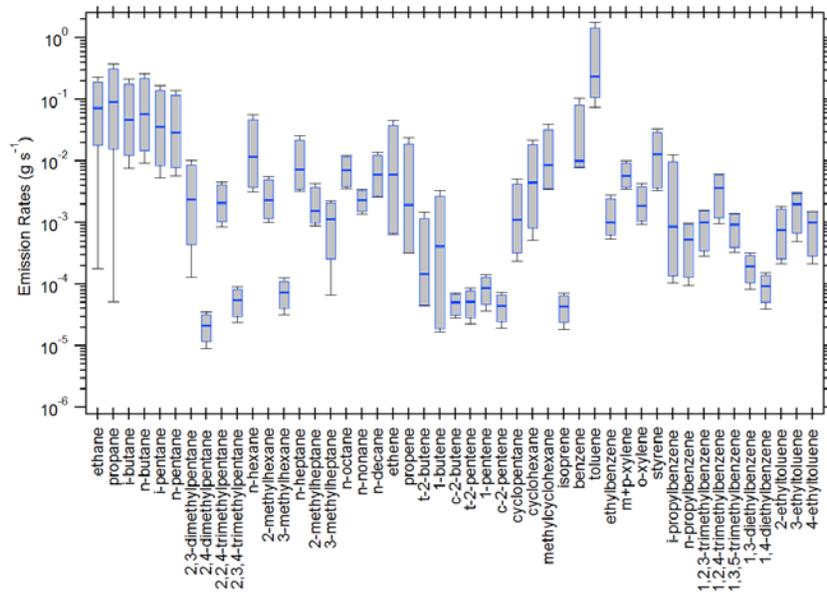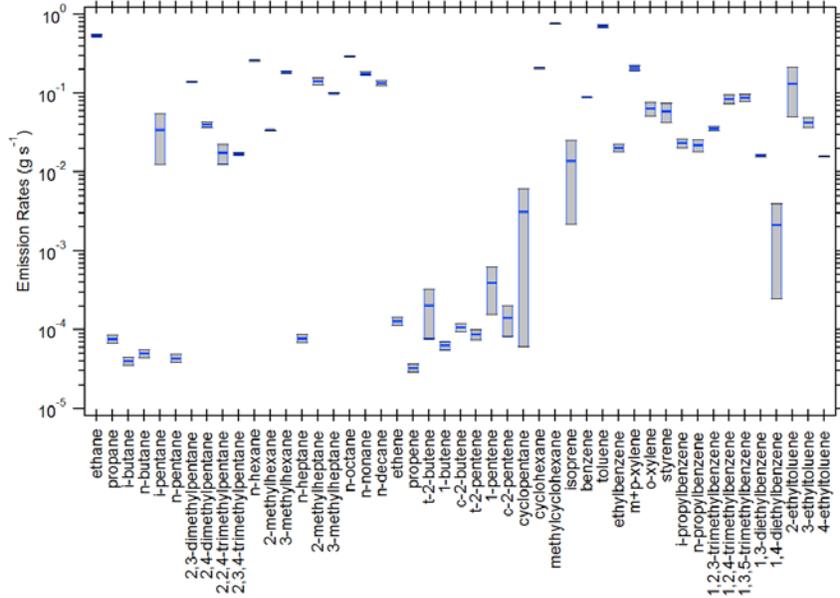
Figure D.4. ERs of VOCs from canisters collected during experiment #5 (drilling; n=4 canisters). The bottom and top of the boxes are the 25th and 75th percentiles, the blue line inside the box represents the median, the bottom and top whiskers are the 5th and 95th percentiles.
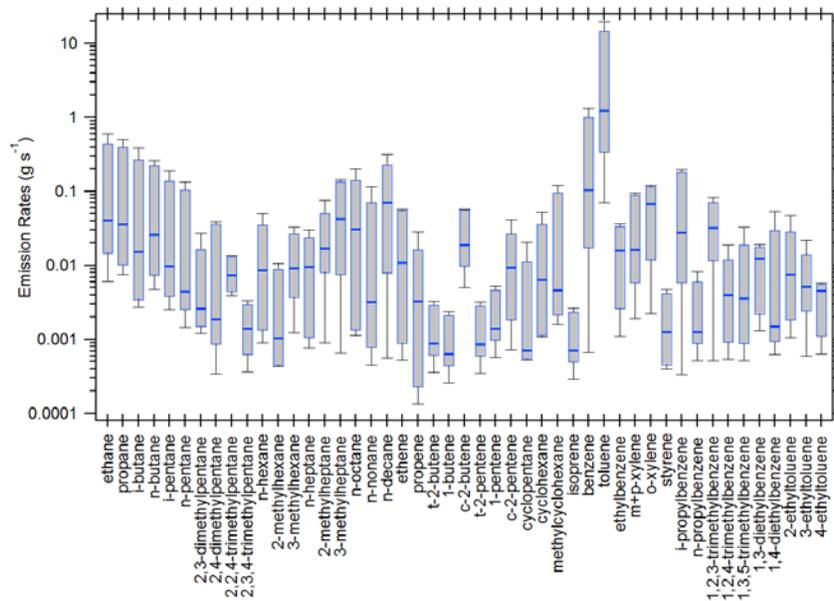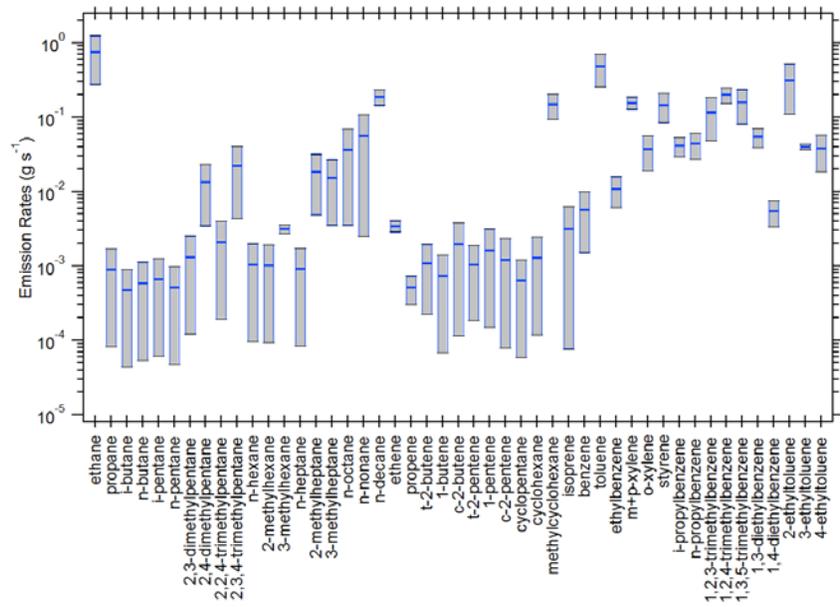

Figure D.5. ERs of VOCs from canisters collected during experiment #6 (remote fracking; n=4 canisters). The bottom and top of the boxes are the 25th and 75th percentiles, the blue line inside the box is the median, the bottom and top whiskers are the 5th and 95th percentiles.

Figure D.6. ERs of VOCs from canisters collected during experiment #7 (fracking; n=17 canisters). The bottom and top of the boxes are the 25th and 75th percentiles, the blue line inside the box represents the median, the bottom and top whiskers are the 5th and 95th percentiles, and the stars are the outliers beyond the 5th and 95th percentiles.
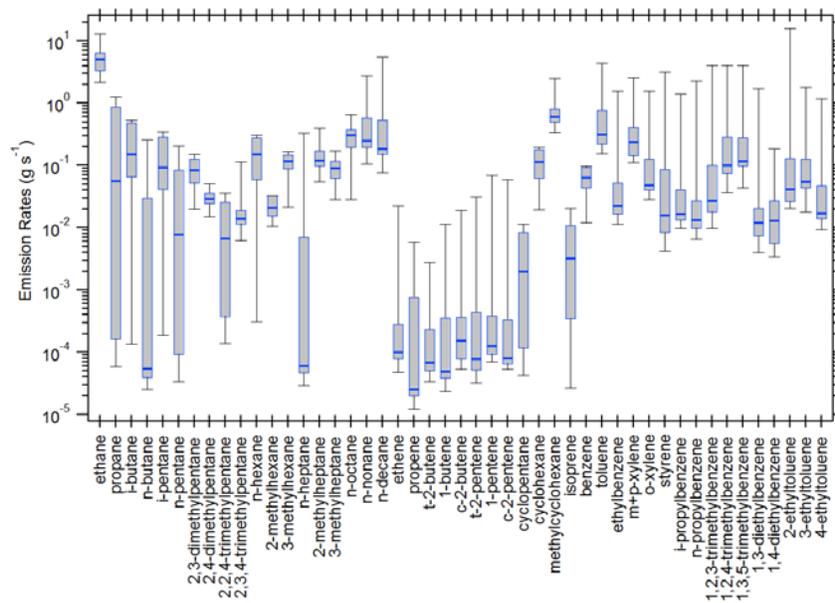

Figure D.7. ERs of VOCs from canisters collected during experiment #8 (flowback; n=21 canisters). The bottom and top of the boxes are the 25th and 75th percentiles, the blue line inside the box represents the median, the bottom and top whiskers are the 5th and 95th percentiles, and the stars are the outliers beyond the 5th and 95th percentiles.

Figure D.8. ERs of VOCs from canisters collected during experiment #9 (fracking; n=1 canister). The bottom and top of the boxes are the 25th and 75th percentiles, the blue line inside the box represents the median, th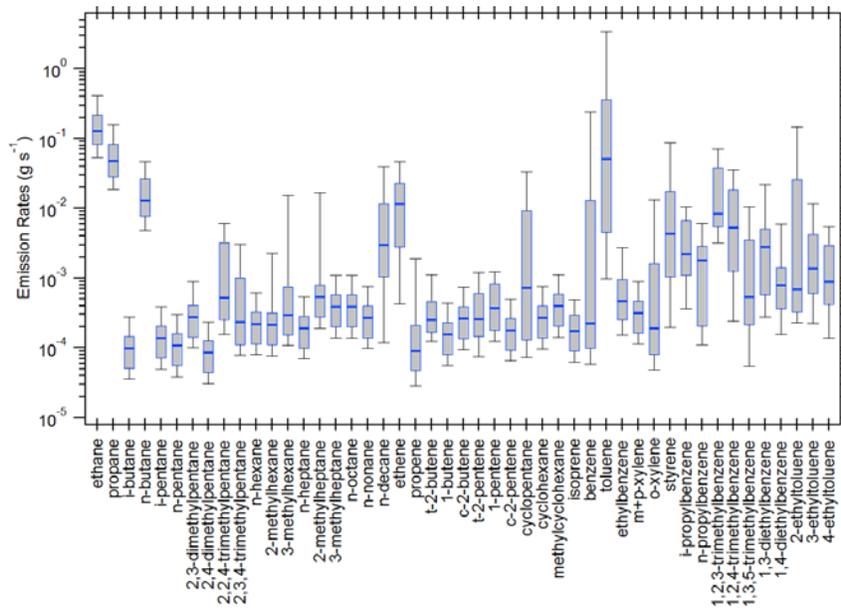e bottom and top whiskers are the 5th and 95th percentiles. Data from 2 canisters are presented as these were the ones that passed the criteria noted in Section 2.3.2.

Figure D.9. ERs of VOCs from canisters collected during experiment #10 (fracking and flowback; n=1 canister). The bottom and top of the boxes are the 25th and 75th percentiles, the blue line inside the box represents the median. Data from 2 canisters are presented as these were the ones that passed the criteria noted in Section 2.3.2.

56

Figure D.10. ERs of VOCs from canisters collected during experiment #11 (flowback; n=9 canisters). The bottom and top of the boxes are the 25th and 75th percentiles, the blue line inside the box represents the median, the bottom and top whiskers are the 5th and 95th percentiles.
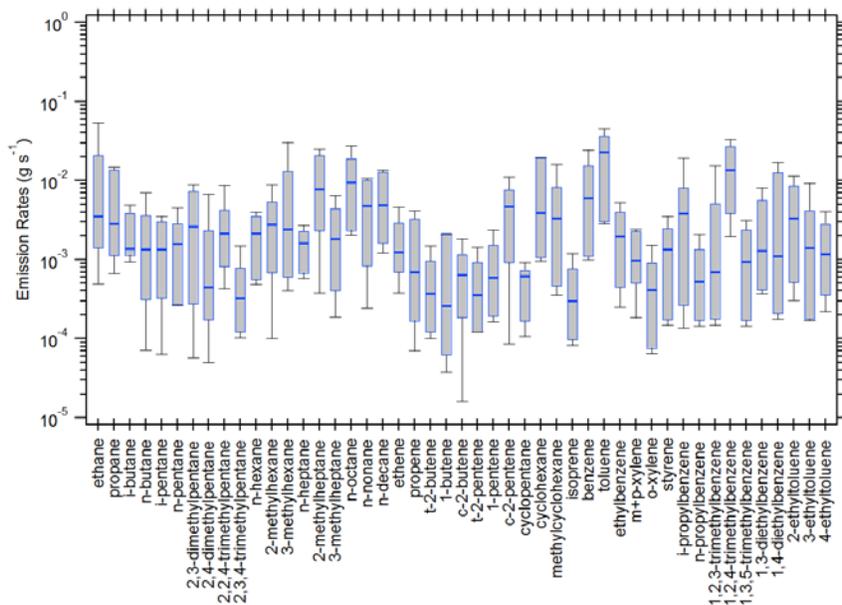

Figure D.11. ERs of VOCs from canisters collected during experiment #12 (drilling; n=12 canisters). The bottom and top of the boxes are the 25th and 75th percentiles, the blue line inside the box represents the median, the bottom and top whiskers are the 5th and 95th percentiles.
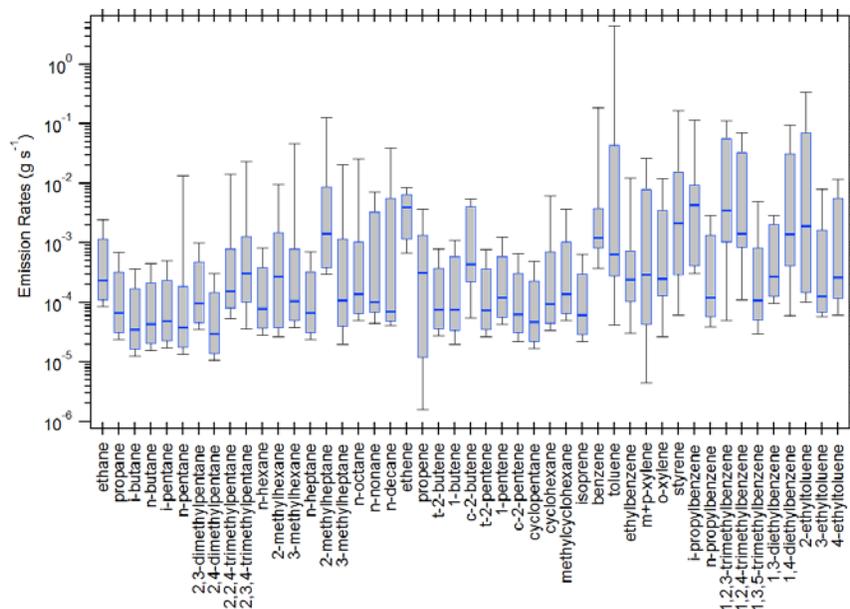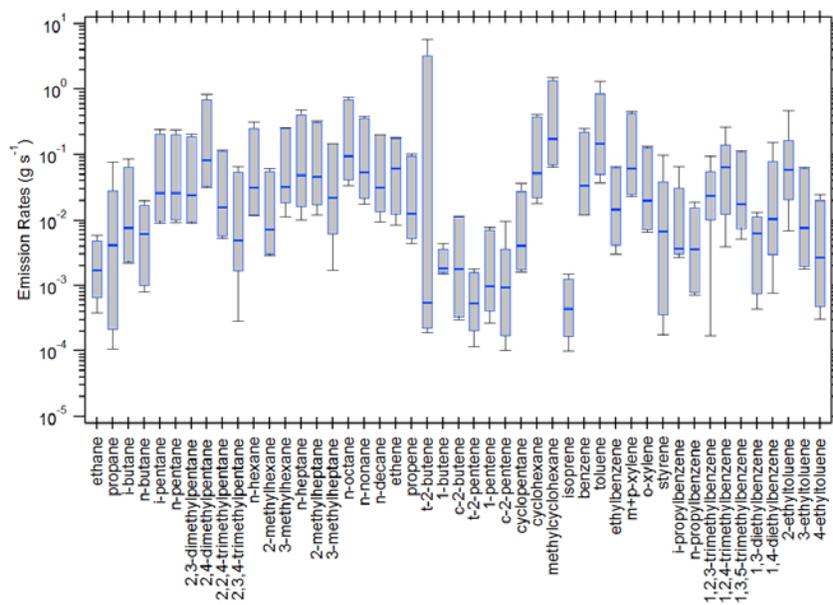
Figure D.12. ERs of VOCs from canisters collected during experiment #13 (drilling, fracking, and flowback; n=9 canisters). The bottom and top of the boxes are the 25th and 75th percentiles, the blue line inside the box represents the median, the bottom and top whiskers are the 5th and 95th percentiles.
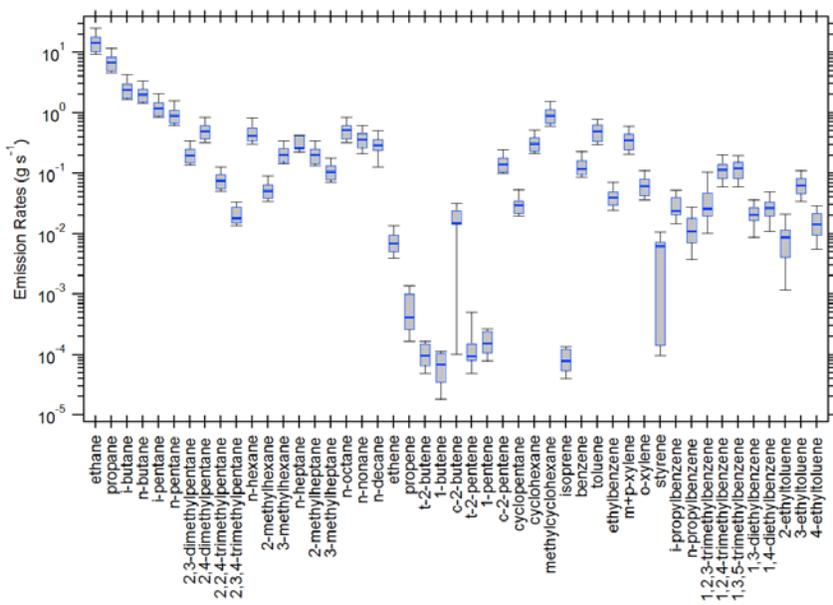

Figure D.13. ERs of VOCs from canisters collected during experiment #14 (fracking; n=9 canisters). The bottom and top of the boxes are the 25th and 75th percentiles, the blue line inside the box represents the median, the bottom and top whiskers are the 5th and 95th percentiles.

Figure D.14. ERs of VOCs from canisters collected during experiment #15 (fracking; n=10 canisters). The bottom and top of the boxes are the 25th and 75th percentiles, the blue line inside the box represents the median, the bottom and top whiskers are the 5th and 95th percentiles.
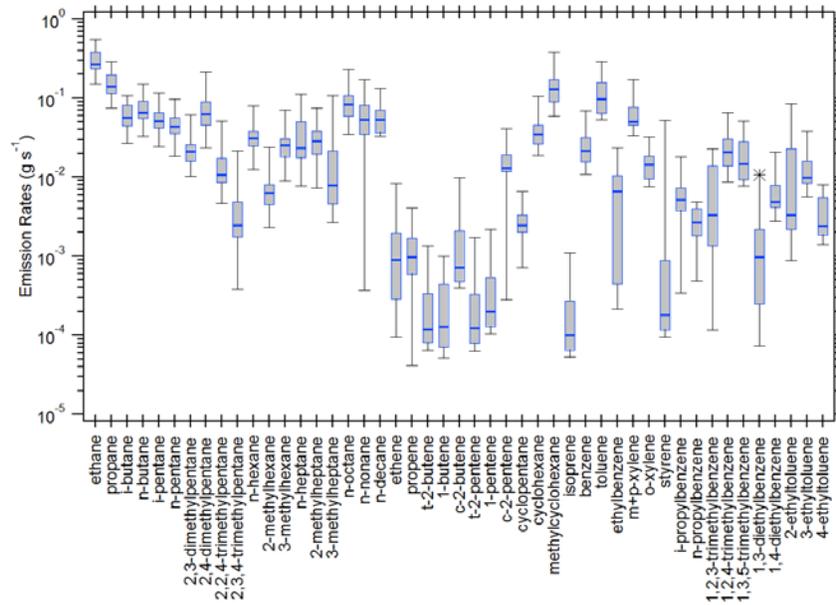

Figure D.15. ERs of VOCs from canisters collected during experiment #16 (flowback; n=11 canisters). The bottom and top of the boxes are the 25th and 75th percentiles, the blue line inside the box represents the median, the bottom and top whiskers are the 5th and 95th percentiles.
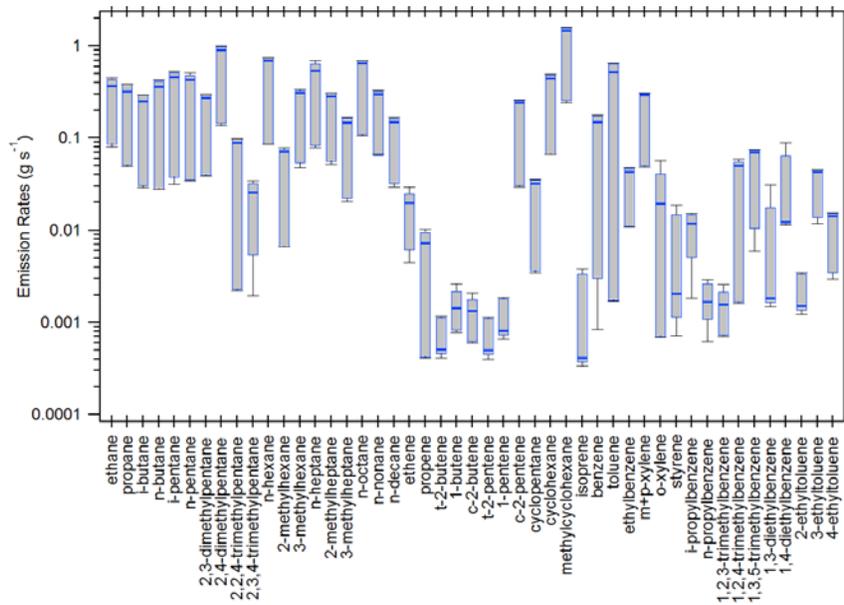
Figure D.16. ERs of VOCs from canisters collected during experiment #17 (flowback; n=15 canisters). The bottom and top of the boxes are the 25th and 75th percentiles, the blue line inside the box represents the median, the bottom and top whiskers are the 5th and 95th percentiles.

Figure D.17. ERs of VOCs from canisters collected during experiment #18 (fracking and flowback; n=5 canisters). The bottom and top of the boxes are the 25th and 75th percentiles, the blue line inside the box represents the median, the bottom and top whiskers are the 5th and 95th percentiles.
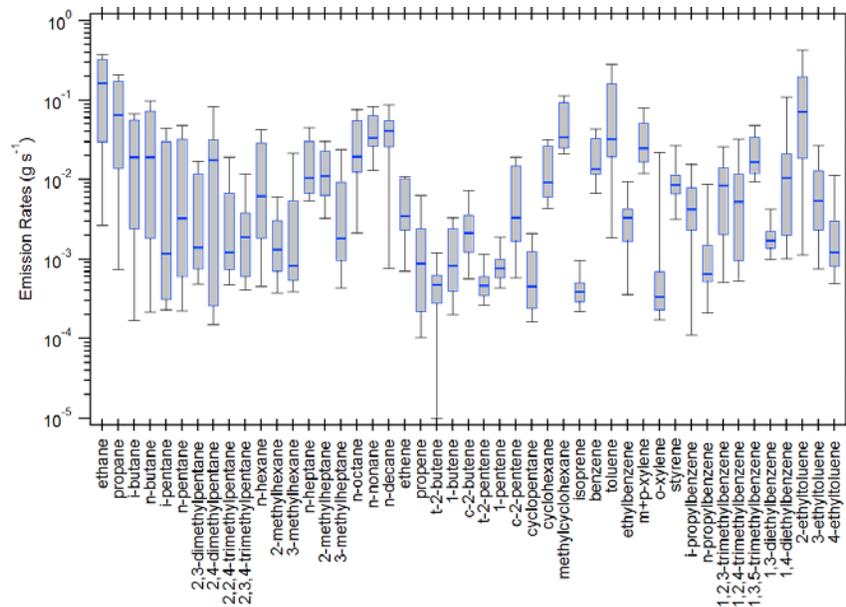
Figure D.18. ERs of VOCs from canisters collected during experiment #19 (flowback; n=18 canisters). The bottom and top of the boxes are the 25th and 75th percentiles, the blue line inside the box represents the median, the bottom and top whiskers are the 5th and 95th percentiles.
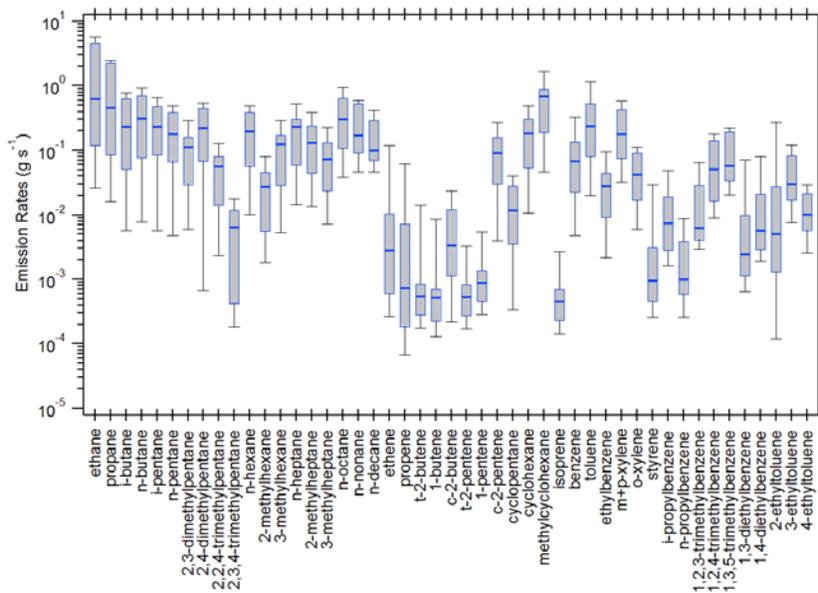

Figure D.19. ERs of VOCs from canisters collected during experiment #20 (flowback; n=12 canisters). The bottom and top of the boxes are the 25th and 75th percentiles, the blue line inside the box represents the median, the bottom and top whiskers are the 5th and 95th percentiles.
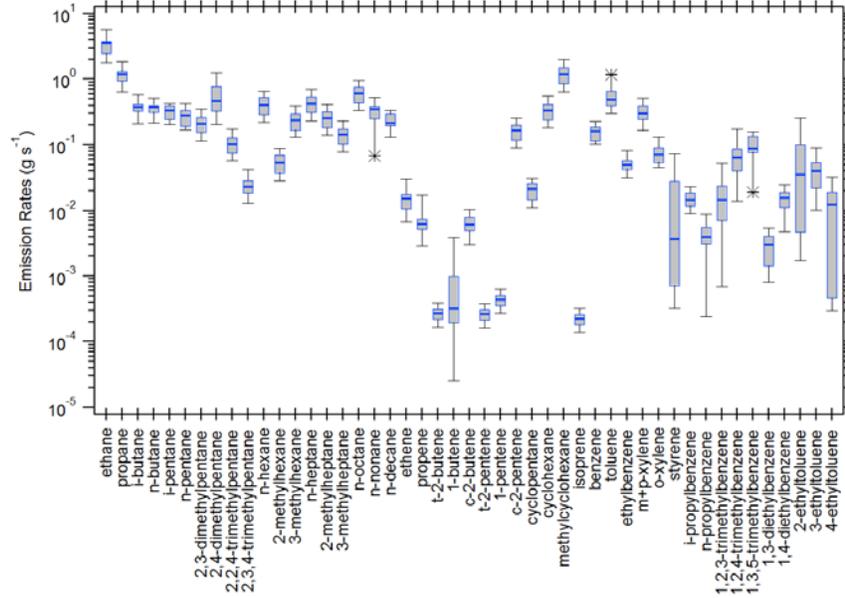
Figure D.20. ERs of VOCs from canisters collected during experiment #21 (fracking and flowback; n=18 canisters). The bottom and top of the boxes are the 25th and 75th percentiles, the blue line inside the box represents the median, the bottom and top whiskers are the 5th and 95th percentiles, and the stars are the outliers beyond the 5th and 95th percentiles.